



# ANNUAL RESEARCH REPORT

## 2021

Gary S. Was, Director  
Ovidiu Toader, Manager and Lead Accelerator Scientist  
Fabian Naab, Senior Accelerator Scientist  
Thomas Kubley, Accelerator Scientist  
Robert Hensley, Electronic Systems Engineer

2600 Draper Road  
Department of Nuclear Engineering and Radiological Sciences  
University of Michigan  
Ann Arbor, Michigan 48109-2145  
[mibl.engin.umich.edu](http://mibl.engin.umich.edu)

Telephone: (734) 936-0131

Fax: (734) 763-4540

## ***The Annual Research Report***

This report summarizes the principal research activities in the Michigan Ion Beam Laboratory during the past calendar year. One hundred and four researchers conducted 40 projects at MIBL that accounted for 121 irradiations and 4204 hours of instrument usage. The programs included participation from researchers at the University, corporate research laboratories, private companies, government laboratories, and other universities across the United States. These projects also included 8 projects funded through the Nuclear Science User Facility program. The extent of participation of the laboratory in these programs ranged from routine surface analysis to triple beam irradiations. Experiments included Rutherford backscattering spectrometry, elastic recoil spectroscopy, nuclear reaction analysis, direct ion implantation, ion beam mixing, ion beam assisted deposition, and radiation damage by proton irradiation and self-ion irradiation, dual ion irradiation and triple beam irradiation. The following pages contain a synopsis of the research conducted in the Michigan Ion Beam Laboratory during the 2020 calendar year.

### ***About the Laboratory***

The Michigan Ion Beam Laboratory for Surface Modification and Analysis was completed in October of 1986. The laboratory was established for the purpose of advancing our understanding of ion-solid interactions by providing up-to-date equipment with unique and extensive facilities to support research at the cutting edge of science. Researchers from the University of Michigan as well as industry and other universities are encouraged to participate in this effort.

The lab houses a 3 MV Pelletron accelerator, a 1.7 MV tandem ion accelerator, and a 400 kV ion implanter that are configured to provide for a range of ion irradiation and ion beam analysis capabilities utilizing 9 beamlines, 5 target chambers and a transmission electron microscope. The control of the parameters and the operation of these systems are mostly done by computers and are interconnected through a local area network, allowing for complete control of irradiations from the control room as well as off-site monitoring and control.

In 2010, MIBL became a Partner Facility of the National Scientific User Facility (NSUF), based at Idaho National Laboratory, providing additional opportunities for researchers across the US to access the capabilities of the laboratory. In 2016, MIBL was recognized as the top ion beam laboratory in the U.S. by the Nuclear Science User Facilities program.

This past year was a difficult one due to COVID that forced closure of the laboratory from mid-March to mid-June, and restricted operation thereafter for several months. Nevertheless, by the end of the year the laboratory was fully operational.

Respectfully submitted,



Gary S. Was, Director

# **Research Projects**

# **Nuclear Science User Facility (NSUF) Projects**

# HIGH FIDELITY ION BEAM SIMULATION OF HIGH DOSE NEUTRON IRRADIATION

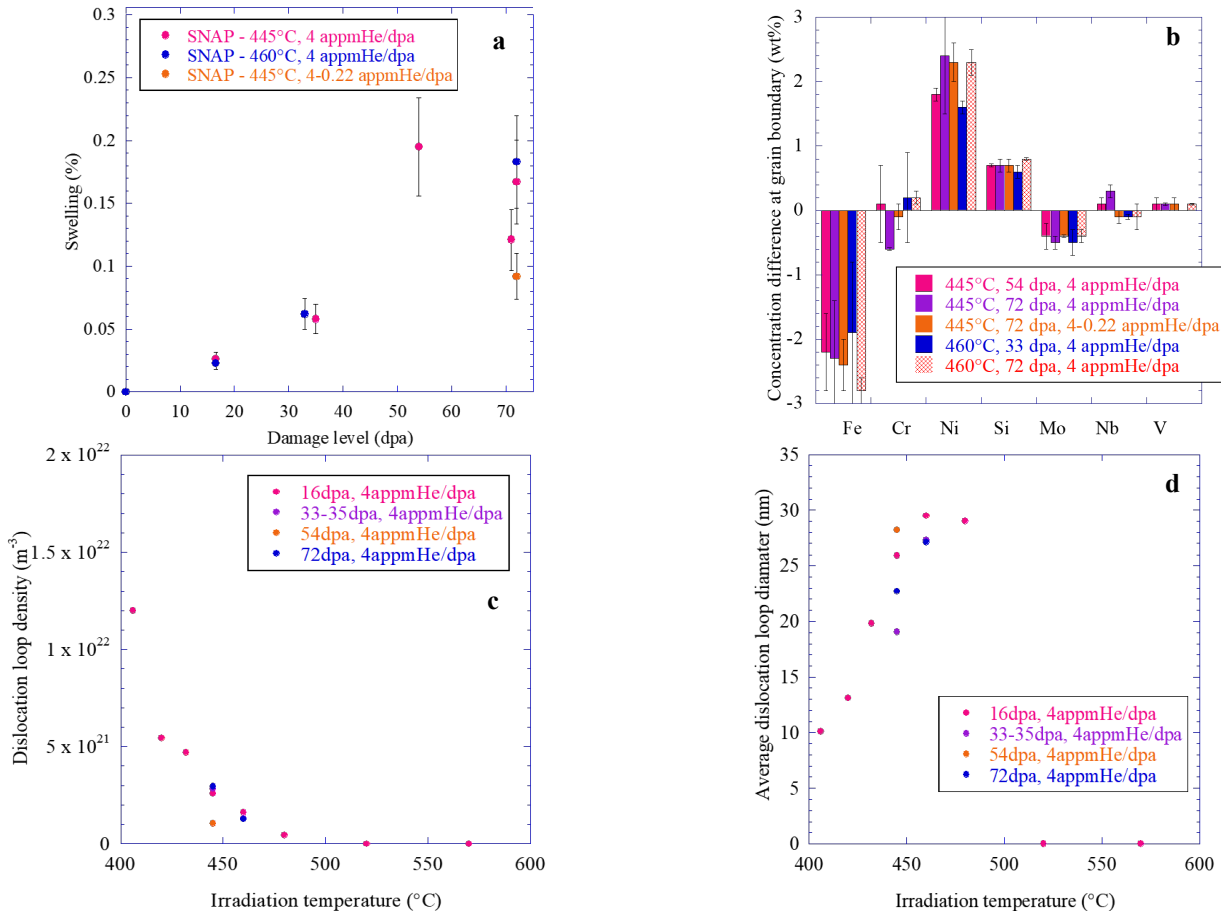
V. Pauly, S. Taller, Z. Jiao, K. G. Field, G.S. Was

Department of Nuclear Engineering and Radiological Sciences, University of Michigan

Traditional research efforts to understand radiation-induced processes in materials requires years of comprehensive post-irradiation characterization effort of neutron irradiated material from test reactors. The same levels of radiation damage can be achieved using heavy ion irradiation under tightly controlled conditions in days or weeks instead of years in a nuclear reactor, albeit with several challenges. The purpose of this work is to address these challenges in using ion irradiation experiments as a surrogate for neutron irradiation.

Several dual ion irradiations were performed using 9.0 MeV defocused  $\text{Fe}^{3+}$  ions to damage the material and simultaneously injecting  $\text{He}^{2+}$  ions to emulate gas buildup from nuclear transmutation reactions. Samples of alloy T91 were dual ion irradiated up to 72 dpa with 4.3 appm helium per dpa at 445 and 460°C and to 72 dpa at 445°C with 4.3 appm He/dpa for the first 35 dpa and 0.22 appm He/dpa for the remaining 37 dpa. These specimens are being examined with transmission electron microscopy to determine the effects of simultaneous helium injection and radiation damage on the irradiated microstructure of these materials.

This work is supported by the U.S. Department of Energy under award DE-NE0000639. This research was performed, in part, using instrumentation provided by the Department of Energy, Office of Nuclear Energy, Nuclear Technology R&D (formerly Fuel Cycle R&D) Program, and the Nuclear Science User Facilities.



Damage level and temperature effect on (a) swelling, (b) radiation-induced segregation, (c) dislocation loop density and (d) average dislocation loop diameter.

# RAPID SIMULATION OF VOIDS SWELLING IN PWR INTERNALS

M. Song<sup>1</sup>, K.G. Field<sup>1</sup>, C. Topbasi<sup>3</sup>, J.T. Busby<sup>2</sup>, G.S. Was<sup>1</sup>

<sup>1</sup>Department of Nuclear Engineering and Radiological Sciences, University of Michigan

<sup>2</sup>Materials Science and Technology Division, Oak Ridge National Laboratory, Oak Ridge, TN

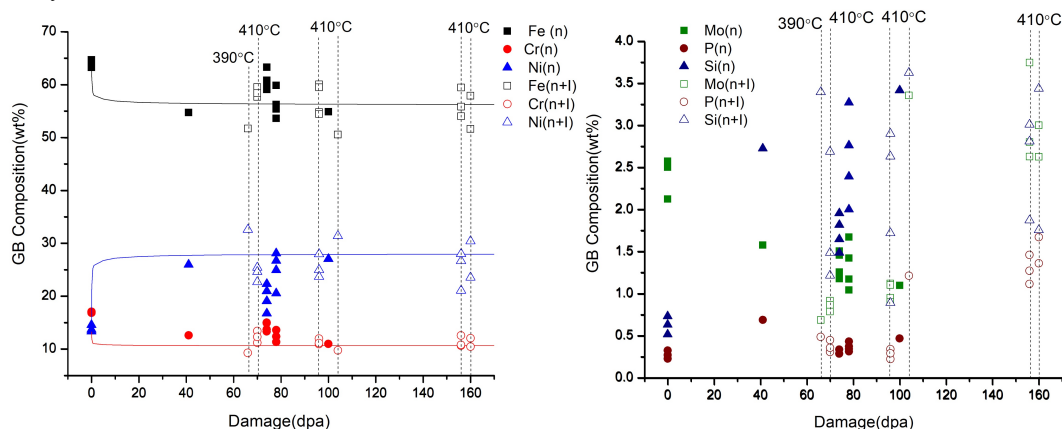
<sup>3</sup>Electric Power Research Institute, Palo Alto, CA

During the past decades, the Electric Power Research Institute (EPRI) has identified void swelling, embrittlement, loss of fracture toughness, and irradiation-assisted stress corrosion cracking (IASCC) as the major degradation mechanisms in light water reactors for long term operation. However, the previous investigation of this project showed that significant dimensional change or void swelling is unlikely in core internals up to 100 dpa when structure materials are in contact with coolant. The other mechanisms remain the concerns for extended operation of nuclear power plants. The goal of this project is to use self-ion ( $\text{Ni}^{3+}$ ) irradiation to continuously capture the microstructure process to ~160 dpa of cold-worked 316L SS after the pre-cursor nucleation processes are completed via PWR irradiations. The monitor of the microstructure changes can provide insight to further potential degradation mechanisms, which are usually tied to irradiated microstructure or shift in microchemistry.

Thin disks with 3 mm in diameter and 0.2 mm thickness were cut from flux thimble tubes of a commercial nuclear power reactor with various neutron damage levels 0, 38-41, 72-75, and 100 dpa. Two irradiation experiments were performed on 38 dpa reactor irradiated samples using Wolverine accelerators with 8 MeV  $\text{Ni}^{3+}$  ions at temperatures of 390 and 410°C to a damage level of 34 dpa, and 72 dpa in total. When compared with reactor irradiated 72 dpa sample, irradiation at 410°C seems a better condition because the major elements match well with the trend of reactor radiation conditions regarding radiation-induced segregation results. Following the same strategy, several reactor irradiated samples were further irradiated to 100 dpa and to 160 dpa at 410°C. The reactor irradiated 38 dpa sample previously irradiated at 410°C was included and irradiated to every dose step to demonstrate the continuous capture of microstructure to 160 dpa.

Radiation-induced segregation, the key to understand IASCC, was used to illustrate the results (shown in Figure). The major elements were consistent with those predicted by the MIK model and within the same damage levels up to 160 dpa despite different neutron and ion dose combinations. Meanwhile, the minor elements were consistent till 100 dpa. The Mo and P in the two 160 dpa samples seemed to be higher than expected. Meanwhile, the nanocavities, dislocation loops, and Ni-Si-rich clusters were also very consistent between neutron and neutron + ion irradiated conditions till 100 dpa. Data on 160 dpa samples are also under analysis.

This work was supported by the Electric Power Research Institute under contract number 10002154 and 10002164 and a grant by the Nuclear Science User Facilities.



Radiation-induced segregation in neutron and neutron+ion irradiated samples to 160 dpa. Dose-dependent GB composition of Left: Major elements and Right: Minor elements. Dpa levels were offset by 4 dpa for ion irradiation conditions for the sake of clarity.

# INVESTIGATION OF IRRADIATION-ASSISTED STRESS CORROSION CRACKING OF ADDITIVELY MANUFACTURED AUSTENITIC STAINLESS STEEL

J.-K. Lee<sup>1</sup>, M. Ickes<sup>2</sup>, O. Toader<sup>3</sup>, G.S. Was<sup>3</sup>

<sup>1</sup>Department of Mechanical Engineering and Materials Science, University of Pittsburgh

<sup>2</sup>Westinghouse Electric Company

<sup>3</sup>Department of Nuclear Engineering and Radiological Sciences, University of Michigan

The goal of this study is to develop the basic understanding of irradiation-assisted stress corrosion cracking (IASCC) in additively manufactured materials. The selected material system is Type 316 austenitic stainless steel which is widely used in parts of nuclear power plant and exhibits IASCC during power plant operation. The design freedom and potential ease of manufacture offered by additive manufacturing (AM) makes this process attractive to reactor engineers, and the implementation of additively manufactured components in nuclear reactors is being pursued by multiple commercial vendors. In comparison to traditional manufacturing, AM of metal powder into bulk metals is known to lead to different microstructures and residual stress. These differences, in turn, are expected to affect the irradiation-induced damage evolution and IASCC of metals. However, there are limited data showing the effect of the manufacturing technique on IASCC. This experiment seeks to utilize the unique microstructures generated by the different additive manufacturing processes to allow for examination of crack initiation behavior in new microstructural environments. This analysis can provide insights into the cracking mechanism.

To examine the effects of manufacturing methods on IASCC, three different kinds of samples were prepared. One method was conventional fabrication – the steel has been hot rolled, cold worked, and machined. The second method was one of AM methods, binder jet printing and sintering using a powder-bed printing system (Invent+, ExOne). The third method was also one of AM methods, selective laser sintering using a laser powder-bed fusion system (M290, EOS). Irradiations experiments were performed at Michigan Ion Beam Laboratory (MIBL) with 2 MeV H<sup>+</sup> ion beams. Single beam (H<sup>+</sup>) irradiations were conducted at 360°C, corresponding to the nominal operation temperatures of Gen-III Light Water Reactors (LWR). The achieved damage was 3 displacement per atom (DPA). In total, 8 tensile bars for slow strain rate testing (SSRT) and 10 bars for transmission electron microscope (TEM) analysis were irradiated. SSRT samples were prepared using a design provided by the University of Michigan. This sample design is compatible with both the accelerator stage fixtures and the CERT loading system at MIBL. The figures (a) and (b) show the photo of a sample stage before irradiation and the thermal image during the irradiation. The irradiation experiment was already completed. After irradiation, the SSRT is being conducted in MIBL at the rate of 10<sup>-7</sup>/s, with half the irradiated samples tested in inert environments, and half the samples tested in simulated PWR conditions.

This work was supported by the U.S. Department of Energy, Office of Nuclear Energy under DOE Idaho Operations Office Contract DE-AC07-051D14517 as part of a Nuclear Science User Facilities experiment.

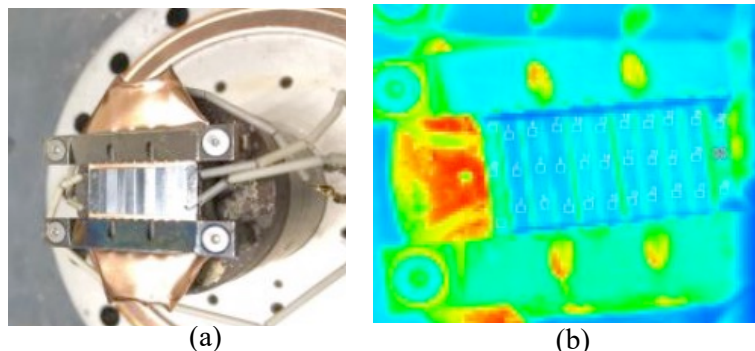


Photo (a) of a sample stage before irradiation, and (b) the thermal image during the irradiation.

# PERFORMANCE AND STRUCTURAL DAMAGE ANALYSIS OF CHALCOGENIDE GLASS PHASE CHANGE TEMPERATURE SENSORS UNDER ION IRRADIATION

A.-A. A. Simon<sup>1</sup>, L. Jones<sup>1</sup>, I. Van Rooyen<sup>2</sup>, M. Mitkova<sup>1</sup>

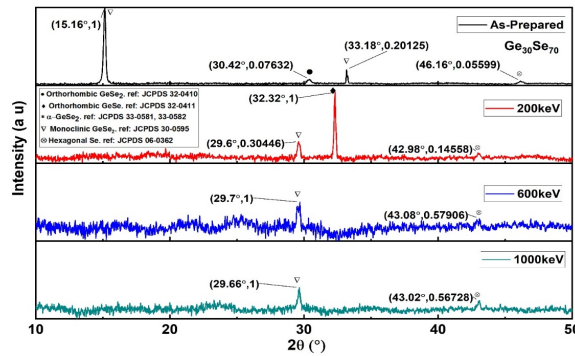
<sup>1</sup>Department of Electrical and Computer Engineering, Boise State University, Boise

<sup>2</sup>Fuel Performance and Design Department, Idaho National Laboratory, Idaho Falls

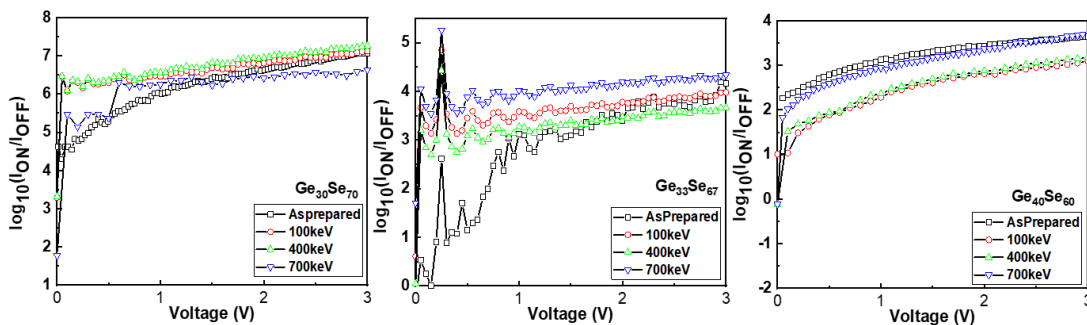
This project is focused on studying the effect of ion irradiation on the crystalline structure of phase change chalcogenide glass (ChG). This is part of testing a new in-situ, reusable and reversible sensor concept which utilizes the amorphous-to-crystalline phase change property of ChG. In this study, for the first time the impact of irradiation on their crystalline structure and I-V characteristics have been studied extensively. New phases have been found to form after irradiation. Moreover, the current-voltage relationship showed that the crystalline structures are able to withstand up to 10dpa and still retains the crystalline structure. More expressed structural changes occur in the crystalline phases which during irradiation change their structure from crystalline GeSe<sub>2</sub> to crystalline GeSe.

To examine the effects of ion damage and irradiation tolerance, thin films and phase change devices were prepared by thermal evaporation of Ge<sub>30</sub>Se<sub>70</sub>, Ge<sub>33</sub>Se<sub>67</sub> and Ge<sub>40</sub>Se<sub>60</sub>. The crystallized thin films and devices were heated to crystallize. The devices were irradiated with Xe<sup>+</sup> ions of energy 100keV, 400keV and 700keV. The total damage was 10 dpa with a total fluence of 1.0 x 10<sup>15</sup> ions/cm<sup>2</sup>. The I-V characteristics showed that after 10 dpa of damage the current is still at the same order of magnitude.

This work was financially supported by the US Department of Energy (DOE), grant number DOE-NE 0008691 and DOE-NSUF RTE award 19-2832.



XRD of irradiated Ge<sub>30</sub>Se<sub>70</sub> crystallized thin films



Current-Voltage characteristics of ion irradiated devices compared to as prepared devices.

# IN-SITU RESISTANCE MEASUREMENTS OF AEROSOL JET PRINTED SILVER UNDER He<sup>++</sup> IRRADIATION

K. Fujimoto<sup>1,2</sup>, T. Unruh<sup>2</sup>, D. Estrada<sup>1</sup>, M. McMurtrey<sup>2</sup>, O. Toader<sup>3</sup>, G.S. Was<sup>3</sup>

<sup>1</sup>Micron School of Materials Science and Engineering, Boise State University

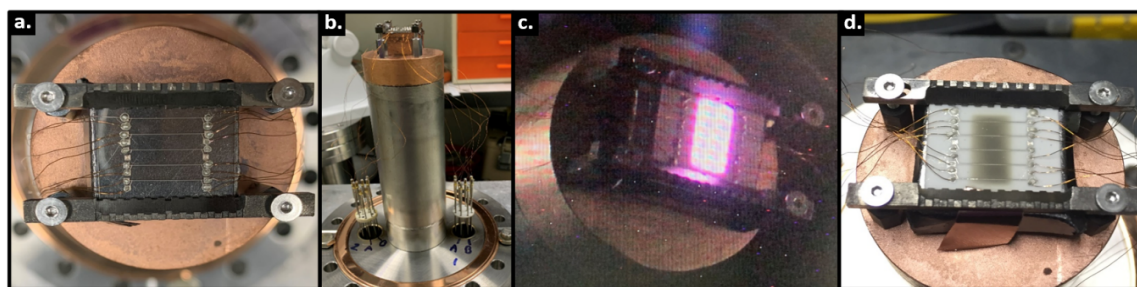
<sup>2</sup>Idaho National Laboratory

<sup>3</sup>Department of Nuclear Engineering and Radiological Sciences, University of Michigan

This work provided the completion of a Rapid Turnaround Experiment (RTE) from 2019 where the effects of He<sup>++</sup> on the electrical resistance of aerosol jet printed (AJP) silver are being investigated. The motivation for these studies is to facilitate a graded approach of rapidly down selecting the library of materials compatible with additive manufacturing techniques for the development of advanced in-pile sensors. Preliminary results for the electrical response of printed silver to He<sup>++</sup> irradiation was a decrease in resistance at 0.01, 0.05 and 0.25 displacements per atom (DPA). However, for this initial study, resistance measurements were performed ex-situ.

Modifications to the initial study included a minimum target of 1.0 DPA, the use of alumina and sapphire substrates to investigate substrate effects, and an experiment set-up that allowed for in-situ resistance measurements to monitor the effects of He<sup>++</sup> irradiation in real-time. These experiments include the use of a four-point structure for electrical characterization, and printing was performed with an Aerosol Jet 200 system. Alumina and sapphire samples were prepared at Boise State University, and began with a pre-processing of both substrates to include O<sub>2</sub> plasma etch at 100 W for 60 sec. Post-processing involved sintering of printed structures at 350 °C for 60 min, and the attachment of 0.1 mm Kapton insulated copper wire with Epotek H20E cured at 120 °C for 15 minutes.

To investigate the irradiation response of He<sup>++</sup> two irradiation experiments were performed using the 1.7 MV Maize Tandem particle accelerator to achieve 1.19 DPA on AJP silver printed on both alumina and sapphire substrates. In-situ resistance monitoring was made possible with the use of custom cables fabricated by MIBL, and by utilizing National Instruments USB-4065 Digital Multimeters. The beam energy was selected to ensure that He<sup>++</sup> ions fully penetrated the printed structures, and temperature control was made with thermocouples to ensure that the irradiation did not exceed 350 °C. An example of the sample set-up can be found in the figures parts a-c. To ensure that only the irradiation effects on printed materials was investigated, an area between the pads was selected for irradiation, which is made visible with the gray area in part c. discoloration of the alumina substrate is a result of the irradiation process, and preliminary analysis exhibits no significant change in device resistance after having experienced a total of 1.19 DPA.



Sample irradiation stage demonstrating (a.) AJP four-point silver structures on sapphire with attached copper wire leads, (b.) attachment strategy for in-situ monitoring of electrical resistance with copper wire leads attached to 10-pin feedthroughs, (c) sample with beam on, and (d) post-irradiation AJP four-point silver structures where the discolored region makes visible the irradiated area of the AJP four-point structures.

# USING ION IRRADIATION TO EXTEND THE DAMAGE LEVEL OF NEUTRON IRRADIATED STAINLESS STEELS

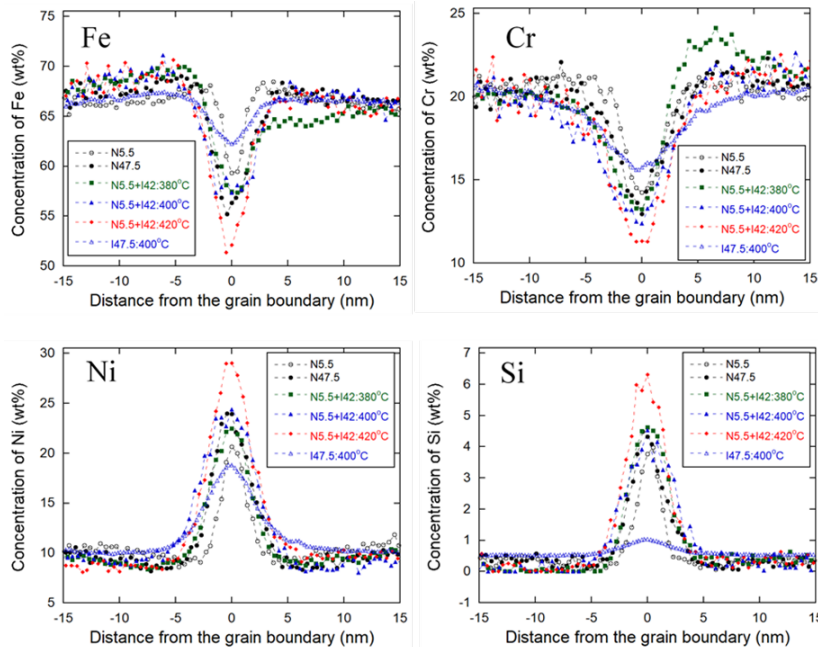
Z. Jiao, S. Levine, M. Song, G.S. Was

Department of Nuclear Engineering and Radiological Sciences, University of Michigan

The objective of this project is to assess the feasibility of re-irradiating existing neutron irradiated alloy 304L SS to high dose levels using ion irradiation, for the purpose of achieving microstructures that represent those from reactor irradiation to those doses. The success of this project would enable the community to evaluate material response at high dose using the existing inventory of reactor-irradiated materials in support of life extension of the current fleet of light water reactors, and the development of high dose radiation-resistant materials for the next generation reactors.

The 304L SS alloy was previously irradiated in the BOR60 reactor to 5.5 dpa at 320°C and was subsequently irradiated with a 9 MeV Ni<sup>3+</sup> ion beam at 10<sup>-3</sup> dpa/s to a dose of 47.5 dpa at 380, 400 and 420°C at MIBL. The irradiated microstructures were compared against those from the neutron irradiated sample at the same dose. As shown in the figure below, combined irradiation (N+I) produced a better match of radiation-induced segregation (RIS) profiles compared to the ion-only irradiation (I47.5) at 400°C. Ion irradiation alone failed to produce the same amount of RIS in this experiment.

This work is supported by the U.S. Department of Energy Nuclear Energy University Program (NEUP) and Nuclear Science User Facilities (NSUF) under grant DE-NE0008520.



Comparison of radiation-induced segregation profiles across the grain boundary in 304L SS at various irradiation conditions.

# VOID SWELLING IN ADDITIVELY MANUFACTURED 316L STAINLESS STEEL UNDER HEAVY IONS

M. Song<sup>1</sup>, X. Lou<sup>2</sup>

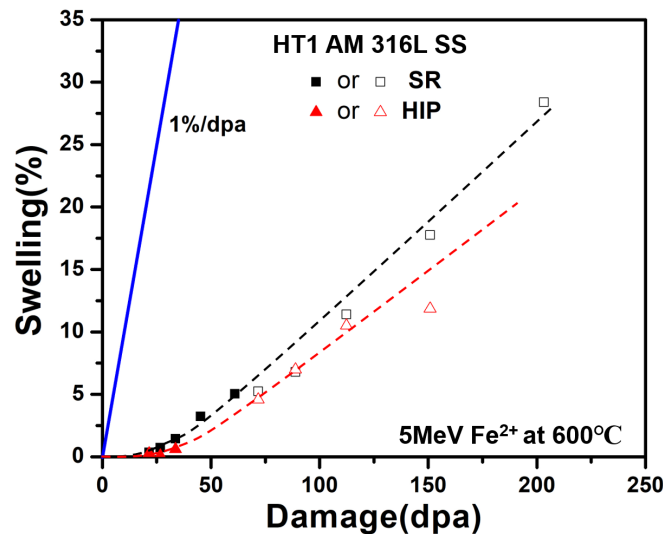
<sup>1</sup>Department of Nuclear Engineering and Radiological Sciences, University of Michigan

<sup>2</sup>Department of Mechanical Engineering, Auburn University

Additive manufacturing (AM) techniques have drawn increasing attention in reactor applications to reduce supply chain, cost, and time to market. The AM techniques were initially considered for producing small parts such as fuel assemblies, control rod drive mechanism, advanced heat exchangers, and debris filter, but were quickly extended to larger parts for core internals and pressure vessels in microreactors or small modular reactors (SMRs) to shorten the lead time and avoid welding. Compared to conventional SSs, the irradiation damage in AM SSs is less explored. Variations in materials processing and irradiation conditions only lead to mixed findings on the radiation tolerance of AM SSs compared to their conventional counterparts.

Two different heat treatments were conducted on the as-printed 316L SS. One is annealing at 650 °C for 2 h, and is referred to as stress-relieved (SR) AM 316L SS. The other is HIP at 1150°C for 4 h with subsequent solution annealing (1066 °C for 1 h), and is referred to as HIP AM 316L SS. These materials were irradiated with 5 MeV Fe<sup>2+</sup> ions to a damage level of 30 or 100 dpa at 600°C using a 3 MV National Electronics Corporation Pelletron accelerator in Michigan Ion Beam Laboratory (MIBL). Void swelling was calculated based on TEM data. The dose-dependent swelling was constructed in the Figure. The incubation dose in HIP AM 316L was slightly higher than that of the SR AM 316L. The steady state swelling rate was similar in the SR AM 316L (0.15%/dpa) compared to HIP AM 316L (0.1%/dpa), both of which were different from the established 1%/dpa for a broad range of neutron-irradiated Fe-Cr-Ni alloys. More details will be available in a journal article.

This work was supported by the U.S. Department of Energy, Office of Nuclear Energy under DOE Idaho Operations Office Contract DE-AC07-051D14517 as part of a Nuclear Science User Facilities experiment, and Nuclear Energy Enabling Technologies Contract DE-NE0008428.



Comparison of swelling with damage levels in AM 316L SS with different post-printing treatments irradiated by 5 MeV Fe<sup>2+</sup> ions at 600°C. Data was carefully selected to avoid both surface effects and injected interstitial effects. Data were extracted from the 300 to 900 nm or 1100 nm range for the HIP or SR samples, respectively. The solid (open) symbols represented for 30 (100) dpa at 600 nm depth or 70 (233) dpa in peak. The dot lines were the visual guide of the swelling curves.

# CRITICAL EVALUATION OF SOLUTE SEGREGATION AND PRECIPITATION ACROSS DAMAGE RATES IN DUAL ION IRRADIATED T91 STEEL

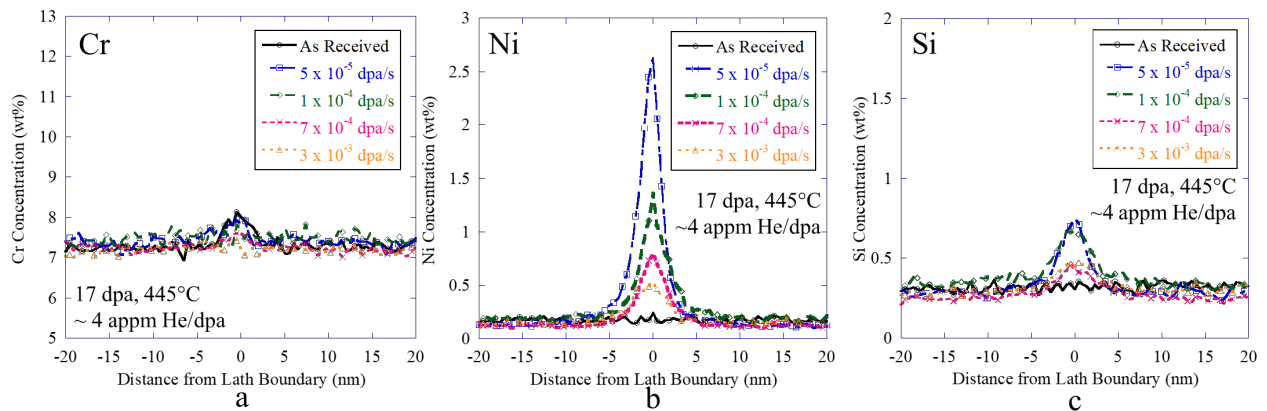
S. Taller, V. Pauly, Z. Jiao, G.S. Was

Department of Nuclear Engineering and Radiological Sciences, University of Michigan

Ferritic-martensitic steels are attractive candidates for structural materials in Gen IV nuclear reactor systems due to their resistance to radiation induced swelling compared to austenitic stainless steels. The strong interaction between solutes and point defects generated during irradiation results in coupled transport of solute atoms by the point-defect fluxes to and away from sinks, such as grain boundaries, free surfaces, dislocation loops, void surfaces, precipitate surfaces, and similar features, leading to radiation induced segregation (RIS) and the formation of secondary precipitates that may be detrimental to the mechanical properties. This work builds on the previous studies by examining the damage rate dependence on both radiation-induced segregation and Ni/Si clustering using dual ion irradiation.

Dual ion irradiations using 5 MeV defocused  $\text{Fe}^{2+}$  ions and co-injected  $\text{He}^{2+}$  ions were conducted on a ferritic-martensitic steel alloy, T91, to 17 dpa at a damage rate range of  $5 \times 10^{-5}$  to  $3 \times 10^{-3}$  dpa/s at 445°C followed by characterization of the microstructure using transmission electron microscopy (TEM) and scanning transmission electron microscopy (STEM). Ni/Si clusters and radiation induced segregation (RIS) were quantified using energy dispersive x-ray spectroscopy (EDS) at each condition and compared with the same material in the as-received condition. No significant Cr segregation was found with dual ion irradiation while Ni and Si enrichments both decreased with increasing damage rate.

This research was performed using funding received from the DOE Office of Nuclear Energy's Nuclear Energy University Programs under contract DE-NE0000639. This work was also supported by the U.S. Department of Energy, Office of Nuclear Energy under DOE Idaho Operations Office Contract DE-AC07-051D14517 as part of a Nuclear Science User Facilities experiment.



Irradiation damage rate effect on the segregation of (a) Cr, (b) Ni, and (c) Si at lath boundaries from dual ion irradiation of T91 to 17 dpa at 445°C.

# **Non-NSUF Projects**

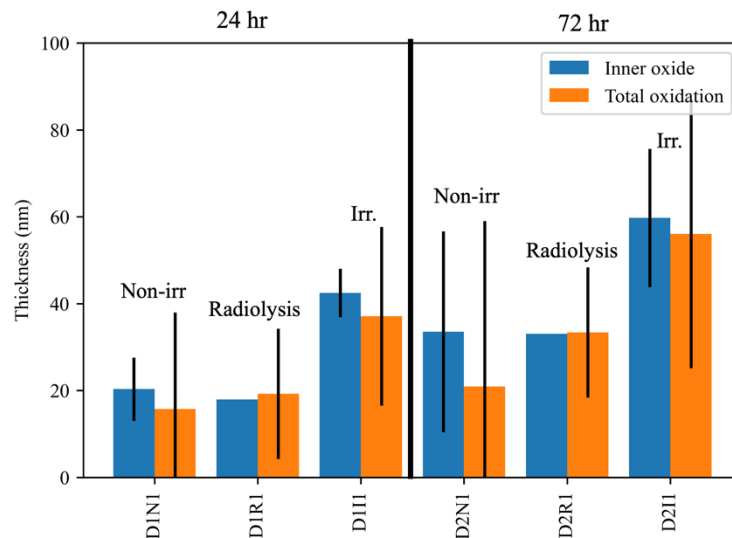
# EFFECTS ON PROTON IRRADIATION ON STEAM OXIDATION OF 316L STAINLESS STEEL

R.D. Hanbury, G.S. Was

Department of Nuclear Engineering and Radiological Sciences, University of Michigan

Two *in situ* proton irradiation corrosion experiments on 316L heat 626032 were completed in the past year. Irradiations were completed using Wolverine, the 3 MV tandem accelerator, on beamline 3. Both irradiation experiments used a 5.4 MeV raster scanned  $H^+$  beam,  $7 \times 10^{-7}$  dpa/s at the corrosion surface,  $<1$  kGy/s water radiolysis in  $480^\circ C$  steam for 24 h and 72 h durations. The steam was generated using inputs of 0.9 L/min Ar-3% $H_2$  as a carrier gas and 0.2 mL/min pure liquid water. Irradiation samples were prepared with a 17-4PH alloy backing plate to reduce sample deformation and radioisotope content and a 316L heat 626032 bar mounted on the sample surface. Both the 316L sample disc and bar were implanted with 400 keV  $He^{++}$  at  $550^\circ C$  to  $10^{16}$  He/cm<sup>2</sup> prior to exposure, producing a bubble marker layer for measuring oxide dissolution [1].

The goal of these experiments is to isolate the effect of displacement damage on corrosion from the radiolysis. The steam environment mitigates the amount of radiolysis that can occur without affecting the displacement damage. Preliminary results show negligible effects of radiolysis on corrosion compared with non-irradiated oxides. Displacement damage causes a definitive increase in corrosion rate in comparison to both radiolysis-affected and non-irradiated oxides. Inner oxide thicknesses are not significantly different from total oxidation measurements, meaning no dissolution occurred as expected in a steam environment.



Measurements of inner oxide thickness and total oxidation for non-irradiated, radiolysis-affected, and fully irradiated regions for both 24 h and 72 h in  $480^\circ C$  hydrogenated steam.

# EFFECT OF HELIUM ON SWELLING IN DUAL-ION IRRADIATED FERRITIC-MARTENSITIC STEELS AT VERY HIGH DAMAGE LEVELS

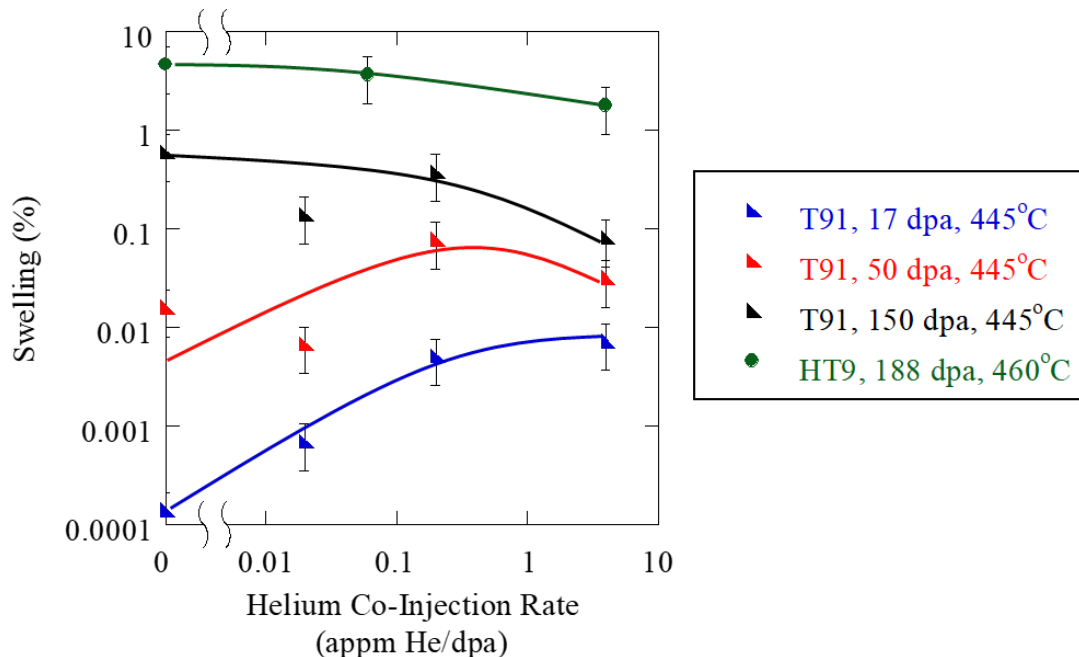
D. Woodley, Z. Jiao, K. Sun, G.S. Was

Department of Nuclear Engineering and Radiological Sciences, University of Michigan

Understanding the microstructural evolution in ferritic-martensitic steels is important for predicting the safety and reliability of future reactors. Dual ion irradiation experiments have been performed on both heat 30176 of T91 and heat 84425 of HT9, two ferritic-martensitic steels, to examine the effects of helium on cavity evolution and swelling at high damage levels. Irradiations were performed at the Michigan Ion Beam Laboratory with 5 MeV  $\text{Fe}^{++}$  ions from a 3 MV Pelletron accelerator and 2.05-2.85 MeV  $\text{He}^{++}$  ions, degraded through a rotating aluminum foil, from a 1.7 MeV Tandetron accelerator to simulate damage and transmutation gas, respectively. Experiments on T91 were performed to 17, 50, 100, 150 and 200 dpa at 445°C with helium-to-dpa ratios of 0, 0.02, 0.22 and 4 appm He/dpa. Experiments on HT9 were performed to 188 dpa at 460°C with helium-to-dpa ratios of 0, ~0.06 and ~4 appm He/dpa. The microstructural behavior was examined using both conventional transmission electron microscopy and scanning transmission electron microscopy. The bubble and cavity behavior were examined for each condition to map out the effect of increased damage level on swelling.

A bimodal size distribution was observed at all damage levels for the conditions in which helium was injected indicating the presence of both bubbles and cavities. At the lowest damage level, the maximum swelling was observed to occur at the highest helium injection rate of 4 appm He/dpa. As the damage level increased, the maximum swelling shifted to lower helium injection rates until at the highest damage levels of 150 and 188 dpa, the maximum swelling was observed to occur without the injection of helium.

This work is supported by the TerraPower, LLC under project N013825.



Swelling in T91, heat 30176, at 445°C and HT9, heat 84425, at 460°C as a function of helium co-injection rate at a variety of damage levels. The lines are there to guide the eye and do not represent trend lines.

# TEMPERATURE-DEPENDENT CAVITY SWELLING IN DUAL-ION IRRADIATED IRON AND IRON-CHROMIUM ALLOYS

Y.-Ru Lin<sup>1</sup>, A. Bhattacharya<sup>2</sup>, D. Chen<sup>3</sup>, Ji-Jung Kai<sup>3</sup>, J. Henry<sup>4</sup>, S. J. Zinkle<sup>1,2</sup>

<sup>1</sup>University of Tennessee, Knoxville

<sup>2</sup>Oak Ridge National Laboratory, Oak Ridge, TN

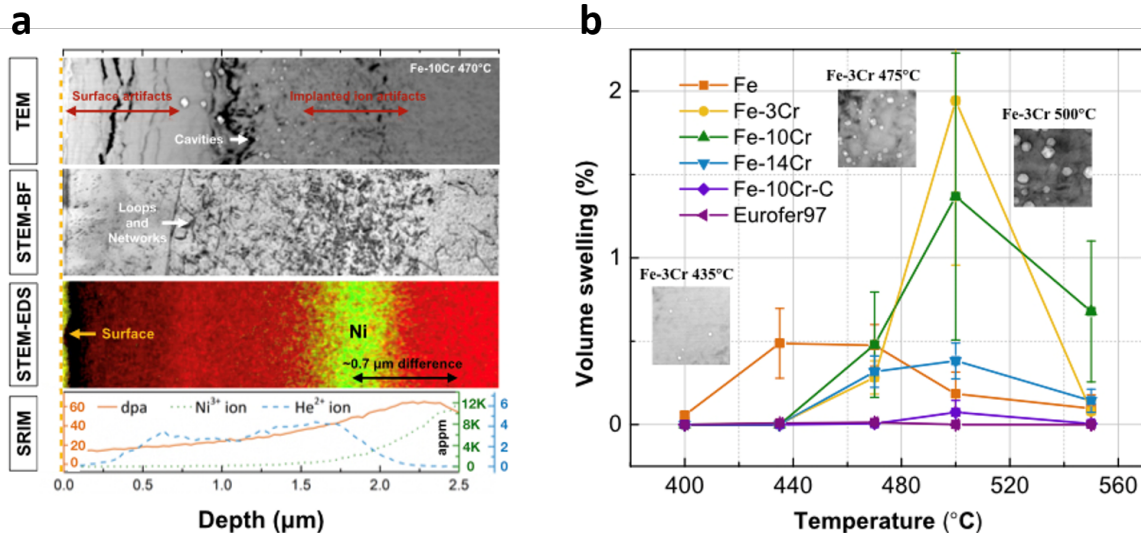
<sup>3</sup>City University of Hong Kong, Hong Kong

<sup>4</sup>CEA, DEN-Service de Recherches Métallurgiques Appliquées, Gif-sur-Yvette, France

The goal of this study is to perform a comprehensive examination of the effect of irradiation temperature and Cr content on cavity swelling, as well as to investigate the microstructural and carbon-induced martensite phase effects on the cavity swelling. Simultaneous dual ion irradiations (8 MeV Ni<sup>3+</sup> ions and energy-degraded 3.55 MeV He<sup>2+</sup> ions) were used to quantify the cavity swelling behavior in ultra-high purity Fe, Fe-Cr alloys, and Eurofer97 steel. The irradiations were conducted over a wide temperature range (400-550 °C) with a mid-range dose of ~30 dpa and 0.1 appm He/dpa implantation rate. The total fluence of the Ni ion beam was  $\sim 9.68 \times 10^{20}$  ions/m<sup>2</sup>. Experiments of 10 appm He/dpa irradiations are in progress.

We reveal that pure Fe has a ~50 °C lower peak swelling temperature difference than Fe-Cr alloys. Cr solute appears to strongly suppress cavity swelling in Fe-Cr alloys for temperatures below ~470 °C, but seems to have little effect or slightly enhances swelling above ~470 °C. Cavities were observed in all the irradiated samples between 400-550 °C. This indicates that the narrow temperature range of observable cavities reported in prior ion irradiated Fe-Cr ferritic alloy studies is likely an artifact associated with the use of low ion energies (<5 MeV), which leads to pronounced near-surface and implanted ion effects that suppress cavity swelling even at midrange depths.

This work was supported by the Office of Fusion Energy Sciences, U.S. Department of Energy under contract DE-AC05-00OR22725 with UT-Battelle, LLC (AB and SJZ) and grant # DE-SC0006661 with the University of Tennessee (YRL and SJZ).



(a) Depth distribution of defects and STEM-EDS mapping of implanted Ni profile in irradiated Fe-10Cr at 470 °C, and SRIM simulation. (b) dependence of cavity swelling on irradiation temperature in dual beam ion irradiated Fe and Fe-Cr alloys.

# PROTON IRRADIATION OF Fe-15Cr MODEL ALLOY

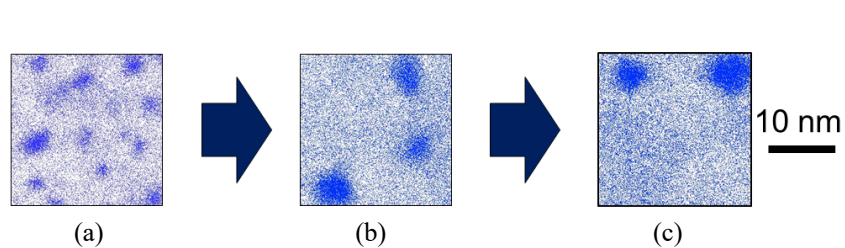
K.N. Thomas, Z. Jiao, G.S. Was

Department of Nuclear Engineering and Radiological Sciences, University of Michigan

High-chromium ferritic-martensitic (F-M) alloys are a candidate materials for future nuclear power plants due to the corrosion resistance and low swelling under irradiation. However, with chromium concentrations above ~9% and at temperatures below ~500°C, the F-M alloys are susceptible to the formation of the Cr-rich  $\alpha'$  precipitates. Research has shown that the  $\alpha'$  precipitates can be formed under thermal aging, as well as neutron, electron, and proton irradiation, but there is difficulty in the  $\alpha'$  precipitate formation under heavy ion irradiation, likely due to ballistic dissolution.

Model alloy Fe-15Cr was irradiated at the Michigan Ion Beam Laboratory (MIBL) in a series of experiments. The 15Cr samples had been previously irradiated with 2 MeV protons to 1 dpa at 400°C at  $1 \times 10^{-5}$  dpa/s to establish an  $\alpha'$  precipitate microstructure. One of the proton irradiated samples was further irradiated utilizing a 1.5 MeV proton beam with a damage rate of  $1 \times 10^{-4}$  dpa/s to 1 and 10 dpa at 400°C. The effects of further proton irradiation with a higher damage rate on  $\alpha'$  precipitates were observed with atom probe tomography, APT. The  $\alpha'$  precipitates were observed to grow in size and Cr concentration, while reducing in number density and volume fraction.

This work is supported by the U.S. Department of Energy under award DE-NE0000639.



Evolution of  $\alpha'$  in Fe-15Cr irradiated with a) 2 MeV protons at  $1 \times 10^{-5}$  dpa/s to 1 dpa at 400°C, b) and subsequently irradiated with 1.5 MeV protons at  $1 \times 10^{-4}$  dpa/s to 1 dpa at 400°C, and c) again with 1.5 MeV protons at  $1 \times 10^{-4}$  dpa/s to 10 dpa at 400°C.

# PROTON IRRADIATION OF Fe-BASED MULTI-PRINCIPAL ELEMENT ALLOYS

M.E. Parry<sup>1,2</sup>, C.D. Judge<sup>1</sup>, W. Jiang<sup>3</sup>, C. Sun<sup>4</sup>, B. Kombaiah<sup>4</sup>, O. Toader<sup>5</sup>, G.S. Was<sup>5</sup>, T.D. Sparks<sup>2</sup>

<sup>1</sup>Irradiated Fuels & Materials Department, Idaho National Laboratory

<sup>2</sup>Department of Materials Science & Engineering, University of Utah

<sup>3</sup>Computational Mechanics & Materials Department, Idaho National Laboratory

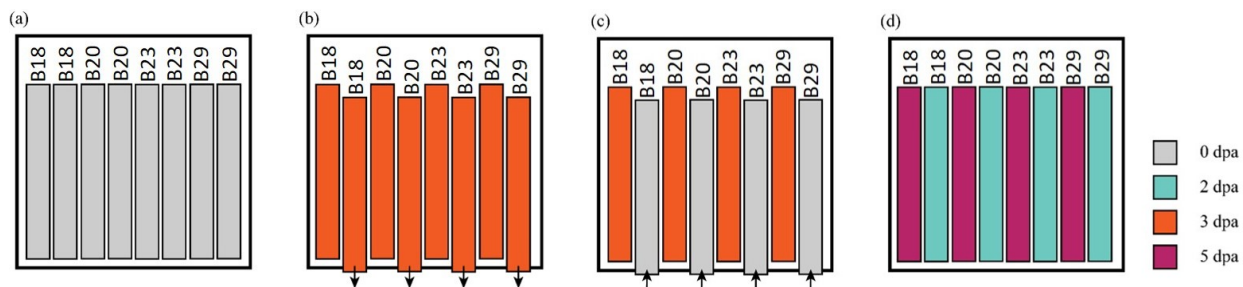
<sup>4</sup>Advanced Characterization Department, Idaho National Laboratory

<sup>5</sup>Department of Nuclear Engineering and Radiological Sciences, University of Michigan

The development of advanced materials with enhanced resistance to irradiation at elevated temperatures is key to the life-extension of advanced nuclear reactors. Fe-based multi-principal element alloys (MPEAs) have desirable thermal and mechanical properties for structural applications in nuclear environments. However, central to the development and implementation of MPEAs as structural materials in reactor applications is an understanding of their thermal and irradiation creep properties. Traditionally, these properties are measured using bulk specimens held at temperature and load for long periods of time. Recent advances in thermal and mechanical testing of irradiated materials creates an opportunity for the accelerated assessment of small-scale specimens which can be linked to engineering-scale data. For instance, experimental setup and accelerator technologies unique to the Michigan Ion Beam Laboratory (MIBL) allow for the efficient study of accelerated degradation mechanisms and creep properties of irradiated materials.

The goal of this study is to evaluate the proton irradiation response in four Fe-based MPEAs, including: FeCrNiMnAl<sub>0.3</sub> (B18), FeCrNiCuAl<sub>0.3</sub> (B20), FeCrNiCuAl (B23), and FeCrNiMnAl (B29). To effectively evaluate creep mechanisms in these materials, the saturation of yield strength due to irradiation must first be understood. Samples were prepared to 2 mm x 2 mm x 20 mm dimensions through cryogenic milling of elemental powders, spark plasma sintering into bulk alloy ingots, electrical discharge machining, and surface polishing to a 3  $\mu\text{m}$  finish. Two irradiations were conducted at MIBL facilities using 2.0 MeV protons, a temperature of 400  $^{\circ}\text{C}$ , an irradiation area of 1.0 cm x 1.6 cm, and to three damage levels: 2, 3, and 5 displacements per atom (dpa). Each irradiation was conducted on 8 samples in the arrangement shown in the Figure, in which half the samples were replaced with pristine samples after irradiation to 3 dpa. The second irradiation to 2 dpa was conducted on 4 samples already at 3 dpa and 4 fresh samples. Completion of both irradiations provided 4 samples at 2 dpa, 4 samples at 3 dpa and 4 samples at 5 dpa. Post-irradiation characterization of hardness and yield strength using nano- and micro-indentation techniques will inform experimental parameters for future irradiation creep tests to be performed at MIBL.

This work was supported through the INL Laboratory Directed Research & Development (LDRD) Program under DOE Idaho Operations Office Contract DE-AC07-05ID14517.



Irradiation scheme. (a) Two of each sample type are placed into chamber, totaling 8 specimens. (b) At temperature, the samples are irradiated to 3 dpa. One of each sample is then removed from the chamber. (c) Along with specimens remaining in the chamber irradiated to 3 dpa, non-irradiated specimens are introduced to the chamber such that two of each sample type are in the chamber. (d) The samples are irradiated to an additional dose of 2 dpa, resulting in samples of 2 dpa and 5 dpa.

# IN-SITU PROTON IRRADIATION-CORROSION EXPERIMENT OF 3C-SiC AT 300°C IN PURE WATER

P. Wang<sup>1</sup>, G. S. Was<sup>1</sup>, L. Czerniak<sup>2</sup>, I. Szlufarska<sup>3</sup>, S.S. Raiman<sup>4</sup>

<sup>1</sup>Department of Nuclear Engineering and Radiological Sciences, University of Michigan

<sup>2</sup>Westinghouse Electric Company

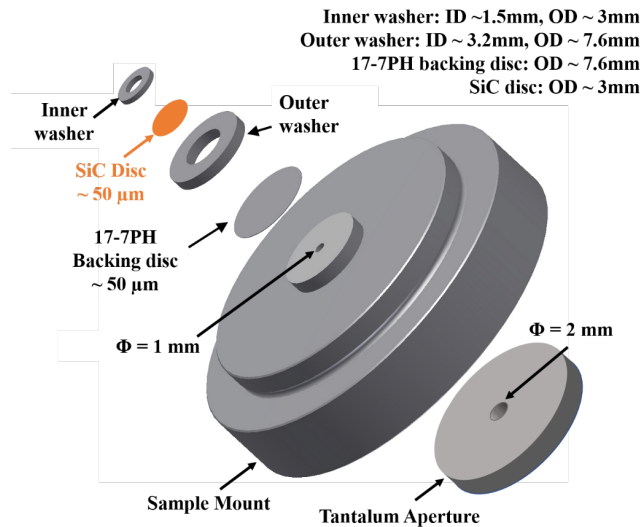
<sup>3</sup>University of Wisconsin, Madison

<sup>4</sup>Oak Ridge National Laboratory

The objective of this project is to develop a mechanistic understanding of the hydrothermal corrosion behavior of monolithic SiC and SiC/SiC composites in the LWR environment under the influence of water radiolysis products and radiation damage. The project focus on the radiation and radiolysis effects of SiC hydrothermal corrosion on chemical vapor deposited (CVD)  $\alpha$ - and  $\beta$ -SiC variants. Specifically, long-term post-irradiation exposures on neutron and ion irradiated samples will be conducted in the LWR temperature regime to evaluate the effect of damage on corrosion kinetics. The effects of water chemistry and radiolysis products on hydrothermal corrosion will be evaluated via in-situ irradiation-corrosion experiments. The extensive post-test characterization will be performed to determine the dissolution rate of the samples, surface morphology, surface chemical composition, and depth profile of SiC from the surface, etc. Activation energies will be determined by fitting dissolution rates to simple empirical relations. Complementary atomistic simulations will be carried out to determine the rate-controlling mechanisms for dissolution under different water chemistries and in the presence of radiation. Activation energies and kinetic rates will be calculated directly from these simulations and they will be compared to experimentally fitted values. The dissolution rate constants determined and validated in this integrated experimental and modeling approach will allow predictions of long-term corrosion behavior of SiC can be predicted.

The figures show a schematic of the sample assembly for the in-situ irradiation-corrosion experiment to study the corrosion response of the SiC disc under proton irradiation in simulated light water reactor conditions.

This research was supported by the Department of Energy, Federal Grant #: DE-NE0008781.



Oxide thickness profile across the in-situ irradiated-corrosion region, the resulting oxide thickness was compared between a coated (data points in blue) and baseline result (dash line in red).

# ASSESSMENT OF SHADOW CORROSION MITIGATION COATINGS USING IN-SITU PROTON IRRADIATION-CORROSION TESTS

P. Wang<sup>1</sup>, G. S. Was<sup>1</sup>, K. Nowotka<sup>2</sup>

<sup>1</sup>Department of Nuclear Engineering and Radiological Sciences, University of Michigan

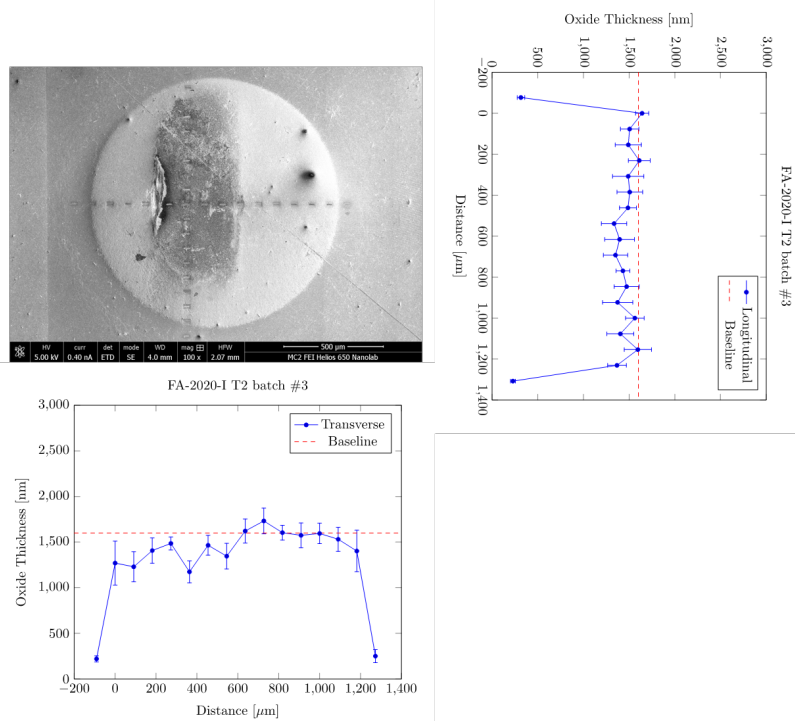
<sup>2</sup>Framatome GmbH

Shadow corrosion is a type of irradiation-assisted galvanic corrosion between dissimilar metals in which the shape of the component is often reproduced in the shape of an area of enhanced corrosion, suggestive of a shadow cast by the component on the zirconium alloy surface. Shadow corrosion is also closely related to the channel bowing phenomena that results in control blade interference due to channel distortion.

Several mechanisms have been proposed to explain the appearance of shadow corrosion and the majority are related to the electrochemical nature of the Zircalloys. However, to date, shadow corrosion has only been observed on samples exposed in reactor. This implies the possible mechanisms by which radiation assists the shadow corrosion process; (1) by increasing the electrical and ionic conductivity of the oxide on Zr alloy, (2) by increasing the oxidizing species at the metal/oxide interface through creating radiolysis products. This project was aimed to use the existing spring-loaded wire design, to assess the durability and effectiveness of the newly developed shadow corrosion mitigation coatings on Inconel 718.

The figure shows that in locations where a shadow corrosion mitigation coating has been applied to the Inconel 718 wire there is no acceleration of oxide growth underneath the Inconel wire. The baseline case represents the oxide thickness resulting from proton irradiation without the Inconel 718 counter-electrode attached.

This research was supported by the Framatome GmbH, Contract No.GF01/1020039285.



Oxide thickness profile across the in-situ irradiated-corrosion region, the resulting oxide thickness was compared between a coated (data points in blue) and baseline result (dash line in red).

# THE INFLUENCE OF ION IRRADIATION ON THE CORROSION KINETICS OF ZIROCNIUM ALLOYS

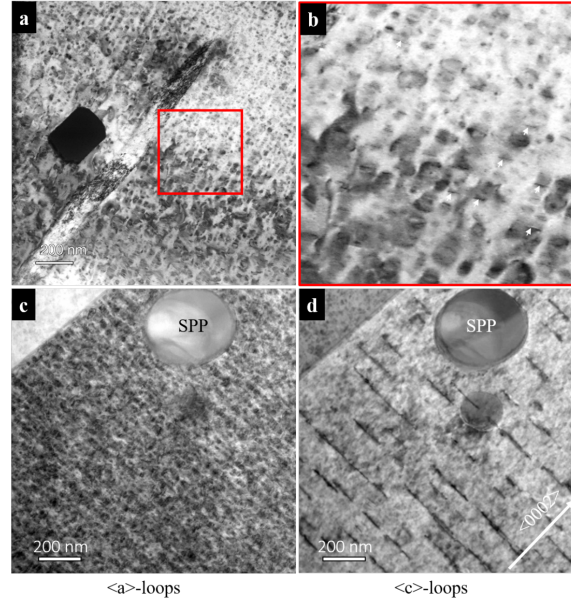
P. Wang<sup>1</sup>, G.S. Was<sup>1</sup>, B. Kammenzind<sup>2</sup>

<sup>1</sup>Department of Nuclear Engineering and Radiological Sciences, University of Michigan

<sup>2</sup>Navel Nuclear Laboratory

The mechanistic understanding of zirconium alloy corrosion in out of reactor testing has advanced the state-of-the-art of the field and provided insights in identifying promising alloys for use in reactors under extreme service duty conditions. However, despite similarities between autoclave and in-reactor corrosion that allow the use of unirradiated material information and testing to identify potential alloys for service, processes that occur in the reactor are quantitatively and qualitatively different than those in an autoclave environment. The aim of this project is to combine ion irradiation (both bulk and in-situ) and advanced characterization techniques to study the effect of irradiation on the corrosion kinetics of zirconium alloys. The research was focused on separate effects testing for the different mechanisms through which irradiation can affect corrosion, namely irradiation induced changes to the base material microstructure and microchemistry, changes to the water chemistry through radiolysis and irradiation effects on the oxide. A set of 2 MeV proton irradiations was carried out on a Zircaloy-4 heat that NNL supplied and a Zr-1Nb alloy from another supplier. Samples with dimension of 2×20×1 mm were irradiated to damage level of 0.5, 1.6 and 5 dpa at temperatures ranging from 250-350°C. A two-step irradiation was also performed on the same alloys to a total of 5 dpa at -10 °C (2.5 dpa) and 350 °C to promote amorphization of the SPP while capturing the dislocation network formation. Fig. 1 shows the STEM images of a completely amorphized SPP and the matrix containing high density of <a>-loops and <c>-loops.

This work was supported by the Navel Nuclear Laboratory.



TEM bright-field image of loops observed on proton irradiated Zircaloy-4, a) -10°C+350°C two-step irradiation to 5 dpa showing the Corduroy effect caused by <a> loop clustering, image was taken from near the <11-20> zone axis, in two-beam  $g=0002$  diffraction conditions, b) zoomed-in image of the area of interest showing some of the edge-on <a> loops appearing as line features, c) <a> loop formation showing Corduroy contrast after 2.5 dpa at 350°C, d) <c> loops edge-on in two beam  $g=0002$  diffraction condition after 2.5 dpa at 350°C.

# A VOID SWELLING RESISTANT TYPE 316L SS DEVELOPED BY ADDITIVE MANUFACTURING ENABLED HIGH THROUGHPUT MICROALLOYING

M. Song<sup>1</sup>, J. Yang<sup>2</sup>, X. Liu<sup>3</sup>, X. Lou<sup>2</sup>, Y. Zhang<sup>4</sup>, L. He<sup>3</sup>, D. Schwen<sup>3</sup>

<sup>1</sup>University of Michigan

<sup>2</sup>Auburn University

<sup>3</sup>Idaho National Laboratory

<sup>4</sup>University of Wisconsin-Madison

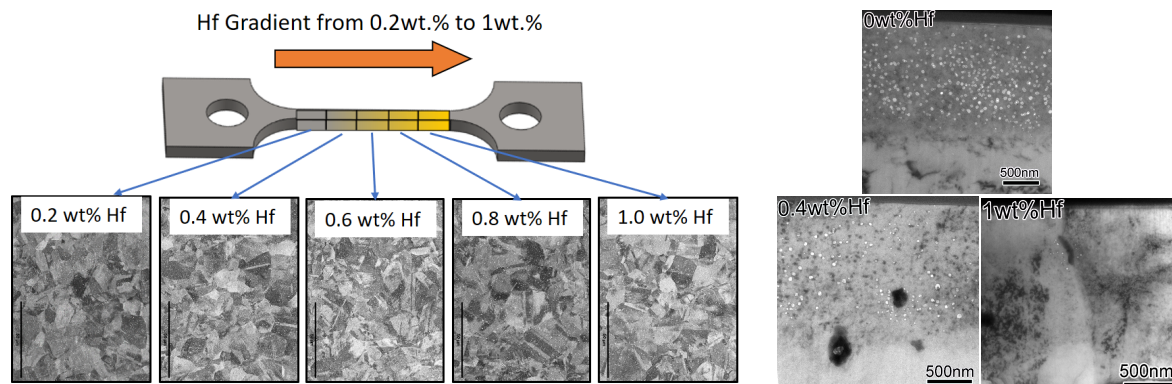
This project demonstrates a rapid alloy design framework for developing reactor structural materials by additive manufacturing. It directly addresses several grand challenges that lead to long and expensive development cycles of nuclear materials, including complex design space, slow manufacturing of nuclear grade samples, and expensive and time-consuming in-pile tests. The proposed approach is being demonstrated by optimization of stainless steels (SSs) for improved resistance to irradiation-assisted stress corrosion cracking (IASCC) for LWRs and swelling resistance for faster reactors.

Microalloyed 316L SS candidates were fabricated by laser additive manufacturing by Auburn University using carefully selected parameters. The modification included four over-sized transition metal elements, Hf, Zr, Y, and Ta. However, only samples with Hf were demonstrated here. As shown in left Figure, through an optimized thermo-mechanical process, the specimen exhibited a similar grain structure as wrought material across the gradient region. The as-built gradient samples were irradiated using 5MeV Fe<sup>2+</sup> ions using a 3 MV National Electronics Corporation Pelletron accelerator in Michigan Ion Beam Laboratory (MIBL). Irradiations were performed at temperatures of 500, 550, 600 °C to a damage level of 50dpa using a raster beam of 8×12 mm<sup>2</sup> with a chamber vacuum pressure under 1×10<sup>-7</sup> torr.

A significant difference in the void structure was observed in the Hf-doped 316L SS samples shown in the right figures. The void density decreased with the increase of Hf. In the 1%Hf doped samples, the voids were smaller in size and lowered in density. The addition of oversized Hf seems to extend the incubation period and delay the steady state void swelling.

At the same time, proton irradiated gradient samples are under evaluation for radiation damage and IASCC susceptibility of the gradient samples.

This work is supported by the Department of Energy, Laboratory Directed Research & Development at Idaho National Laboratory under contract 19A39-071FP.



Gradient 316L SS produced by additive manufacturing and void structure after 50dpa irradiated at 550°C

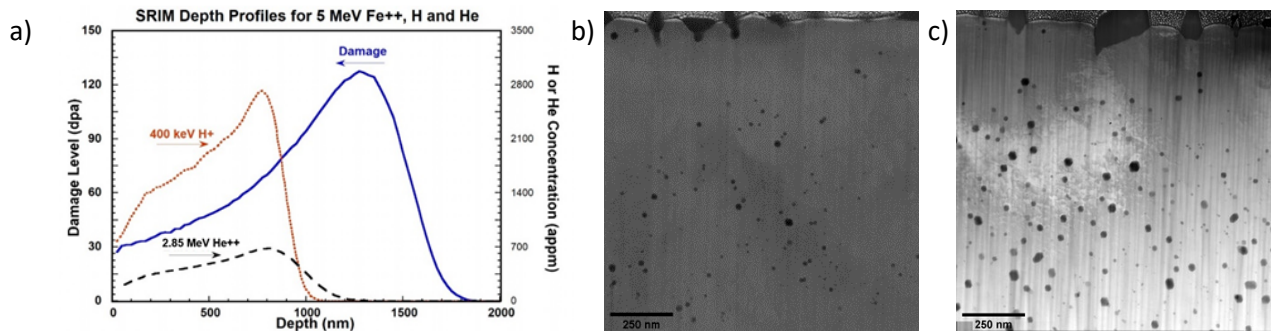
# RESPONSE OF CANDIDATE FUSION BLANKET MATERIALS TO DUAL AND TRIPLE ION IRRADIATION TO UNDERSTAND THE SYNERGIES BETWEEN H, He AND RADIATION DAMAGE

L.N. Clowers<sup>1</sup>, Z. Jiao<sup>1</sup>, F. Naab<sup>1</sup>, T. Kubley<sup>1</sup>, G.S. Was<sup>1</sup>

<sup>1</sup>Department of Nuclear Engineering and Radiological Sciences, University of Michigan

The goal of this study is to investigate the nucleation and growth of cavities and bubbles using multiple ion beams to capture the production of gasses by transmutation in ferritic alloys for fusion blanket materials. The role of H in the nucleation and growth of He bubbles into cavities remains largely unanswered and poorly understood and is critical to assessing performance of candidate alloys for a fusion blanket and first-wall environment. Such behavior will affect the evolution of the irradiated microstructure and could accelerate processes such as He bubble nucleation, transformation of bubbles to cavities and even cavity growth. To investigate these phenomena, a series of irradiations was conducted on three reduced activation ferritic/martensitic (RAFM) steels; F82H (IEA heat from the National Institutes of Quantum and Radiological Science and Technology in Japan), CNA3 (from ORNL) and Fe8Cr2W (made at Ames laboratory). Ion irradiations were conducted at the Michigan Ion Beam Laboratory (MIBL) using the 3 MV Pelletron accelerator to provide a defocused beam of 5 MeV Fe<sup>2+</sup> for irradiation damage, the 1.7 MV Tandetron to provide a raster-scanned beam of 2.85 MeV He<sup>2+</sup> to be passed through a ~6.4 μm thick Al degrader foil for helium implantation, and the implanter to provide a raster-scanned beam of 400 keV H<sup>+</sup> through a second ~2.3 μm Al degrader foil for hydrogen implantation. Samples were irradiated in the multi-beam chamber (MBC), seen in figure (a) with three types of ion irradiation; single ion beam (Fe<sup>2+</sup>), dual ion beam (Fe<sup>2+</sup>+He<sup>2+</sup>), and triple ion beam (Fe<sup>2+</sup>+He<sup>2+</sup>+H<sup>+</sup>) were each conducted at 450°C and 500°C to a damage level of 50 dpa. The damage profiles from self-ions and the concentration profiles of injected H/He calculated using a custom MATLAB script along with SRIM-2013 are shown in figure (a). The appm/dpa ratios for helium and hydrogen are 40 appm/dpa and 10 appm/dpa, respectively, at the depth of analysis (500-700nm from the surface). Helium reached 2000 appm and hydrogen reached 500 appm in the region of interest at the end of 50 dpa irradiation at a damage rate of ~1x10<sup>-3</sup> dpa/s. Thermocouple measurements were used to calibrate the thermal imaging for the temperature determination and were recorded along with pressure and beam current during these irradiation experiments. Post-irradiation microstructural characterization was subsequently performed on focused ion beam (FIB) lift-outs of the irradiated materials via transmission electron microscopy at the Michigan Center for Materials Characterization (MC<sup>2</sup>). The cavity microstructure of F82H after irradiation is shown in figure (b) where the co-injection of H<sup>+</sup> in these irradiations was observed to cause as much as a two-fold increase in the void swelling of each of these alloys at 500°C through enhanced cavity growth when compared to traditional dual ion irradiation.

This material is based upon work supported by the U.S. Department of Energy, Office of Science, Office of Fusion Energy Sciences under Award Number DE-SC0020226.



Displacement and implantation curves for 5 MeV Fe<sup>2+</sup> and energy degraded He<sup>2+</sup>/H<sup>+</sup> in F82H RAFM steel (a). STEM-HAADF images of dual ion (b) and triple ion (c) irradiated F82H at 500°C

# RADIATION TOLERANCE OF ADDITIVELY NANOSTRUCTURED ALLOY-2 (ANA2) FOR ADVANCED REACTORS

T.M. K. Green<sup>1</sup>, K.G. Field<sup>1</sup>, W. Zhong<sup>2</sup>, L. Tan<sup>2</sup>

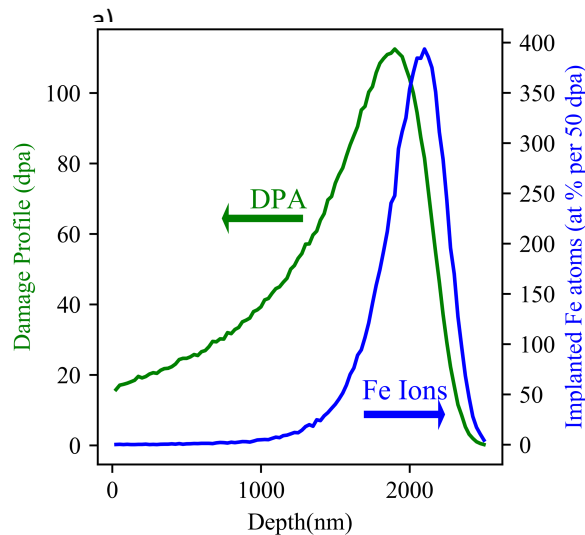
<sup>1</sup>Department of Nuclear Engineering and Radiological Sciences, University of Michigan

<sup>2</sup>Oak Ridge National Laboratory

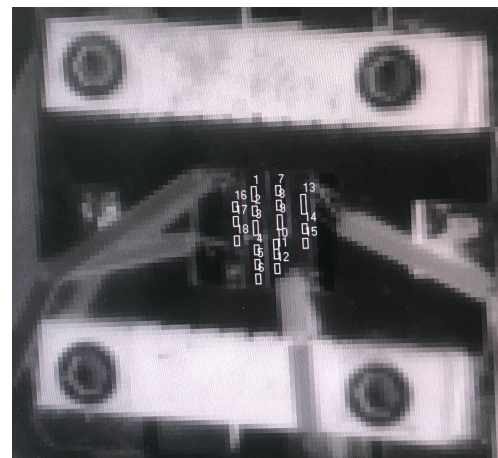
The goal of this multi-year project is to examine the precipitate stability of a new ferritic/martensitic (F/M) alloy designated as Additively Nanostructured Alloy-2 (ANA2) under irradiation and helium bombardment. ANA2 was designed using computational thermodynamics specifically for advanced nuclear reactor environments and was fabricated via the direct energy deposition (DED) additive manufacturing method. It contains  $2.5 \times 10^{22} \text{ m}^{-3}$  of MX-type precipitates in the unirradiated state (Zhong et al. 2021). This particular study was the first in a series of heavy ion irradiations to test the temperature dependence of the MX precipitates in order to isolate the role of temperature on their stability. ANA2's radiation tolerance will be compared to other F/M alloys that undergo the same irradiation conditions.

Four samples of F/M steel bars each  $10^L \times 1.5^H \times 1.5^W \text{ mm}^3$  were machined from bulk specimens of ANA2, F82H, HT9, and Grade 91. The samples underwent a single beam irradiation at  $400^\circ\text{C}$  using  $9 \text{ MeV Fe}^{3+}$  ions at a dose rate of  $1 \times 10^{-4} \text{ dpa/s}$ . Figure (a) below shows the damage profile, in which a total dose of 50 displacements per atom (dpa) at 1,200 nm depth was collected with a total fluence of  $1.16 \times 10^{17} \text{ ions/cm}^2$ . Thermocouples were spot-welded to reference guide bars immediately next to the samples of interest and provided consistent temperature control during the irradiation. The thermocouple measurements were also used to calibrate thermal imaging for temperature determination of the bars during irradiation. Figure (b) shows the sample stage. Pressure, temperature, and beam currents were recorded during the irradiation experiments.

Research and development efforts associated with the DED technology was supported by the Laboratory Directed Research and Development Program of Oak Ridge National Laboratory (ORNL) and the U.S. Department of Energy (DOE), Office of Nuclear Energy (NE), Advanced Fuels Campaign, under Contract with UT-Battelle, LLC. Samples from these efforts were procured, irradiated, and characterized as part of an FES sponsored Early Career Award (DE-SC0021138).



(a)



(b)

Displacement and implantation curves for  $9 \text{ MeV Fe}^{3+}$  (a), and thermal image of the irradiation stage (b).

# DOSE AND SINK STRENGTH DEPENDENCE OF RADIATION INDUCED PRECIPITATES AND SWELLING IN ADDITIVELY MANUFACTURED HT9 FERRITIC/MARTENSITIC STEELS

P. Xiu<sup>1</sup>, N. Sridharan<sup>2</sup>, K.G. Field<sup>1</sup>

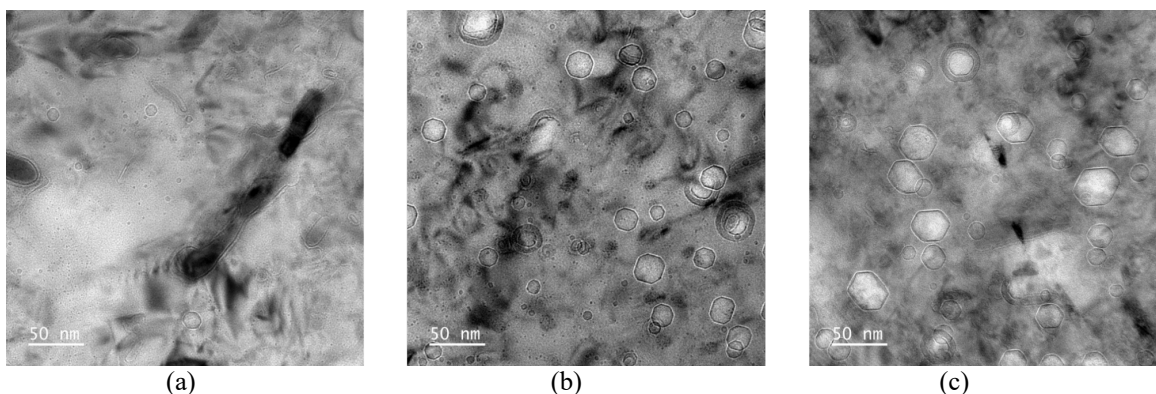
<sup>1</sup>Department of Nuclear Engineering and Radiological Sciences, University of Michigan

<sup>2</sup>Lincoln Electric-India, India

Ferritic martensitic (FM) steels are promising candidate materials for high-dose applications in advanced nuclear reactors due to their low swelling rates. Radiation induced precipitates and swelling are known to degrade the mechanical properties thus affect the performance of FM steels as structural components. The use of additive manufacturing, which includes powder-blown laser directed energy deposition (DED), is gaining more attention for consideration in the production of commercial nuclear reactor components. Additionally, post-built heat treatments can alter the final microstructures of a DED produced component and in turn the sink strength. The result is a possible variance in radiation response of additively manufactured FM steels. Here, a systematic study of additively manufactured HT9 (AM-HT9) alloys is conducted to investigate how sink strength affects AM-HT9's responses to advanced nuclear reactor like conditions including trends as a function of increasing radiation doses.

AM-HT9 samples were produced using powder-blown laser DED at Oak Ridge National Laboratory's Manufacturing Demonstration Facility (MDF) and then processed using two heat treatments that mimic those used in traditional processing routes called ACO3 and FCRD. After that, the as-built (ASB), ACO3 and FCRD samples were dual ion-beam irradiated at the Michigan Ion Beam Laboratory (MIBL) to a total damage dose of 16, 50, 75, 100, 150 displacements per atom (dpa) with 4 He appm/dpa at 445°C. The under-focus TEM images in the Figure show extensive growth of cavities in ACO3 and FCRD, both of which are heat treated with much decreased sink strengths. The ASB sample with a higher sink strength however, primarily exhibited nucleation while quite limited growth of cavities, which suggested a longer incubation period and much higher damage level required for the ASB sample to reach the steady-stage cavity swelling regime. The results indicated that the AM fabrication process and post-built heat-treatments have significant impact on the microstructural evolution and radiation responses in the HT9 alloys.

A portion of the irradiations were supported by the U.S. Department of Energy, Office of Nuclear Energy (DOE-NE), through Nuclear Science User Facilities project 18-1491. Preliminary characterization was supported by the Advanced Fuels Campaign - Nuclear Technology Research and Development program by the US Department of Energy, Office of Nuclear Energy under sub-contract 4000175183 through Oak Ridge National Laboratory.



Under-focus TEM-BF images of irradiated (a) ASB, (b) ACO3 and (c) FCRD after dual beam irradiated to 150 dpa with 4 He appm/dpa at 445°C.

# CORROSION OF PHASE AND PHASE BOUNDARY IN PROTON-IRRADIATED 308L STAINLESS STEEL WELD METAL IN SIMULATED PWR PRIMARY WATER

X. Lin<sup>1,2</sup>, Q. Peng<sup>1,3</sup>, J. Mei<sup>3</sup>, E.-H. Han<sup>1</sup>, W. Ke<sup>1</sup>, L. Qiao<sup>4</sup>, Z. Jiao<sup>5</sup>

<sup>1</sup>Key Laboratory of Nuclear Materials and Safety Assessment, Institute of Metal Research, Chinese Academy of Sciences, China

<sup>2</sup>School of Materials Science and Engineering, University of Science and Technology of China

<sup>3</sup>Suzhou Nuclear Power Research Institute, China

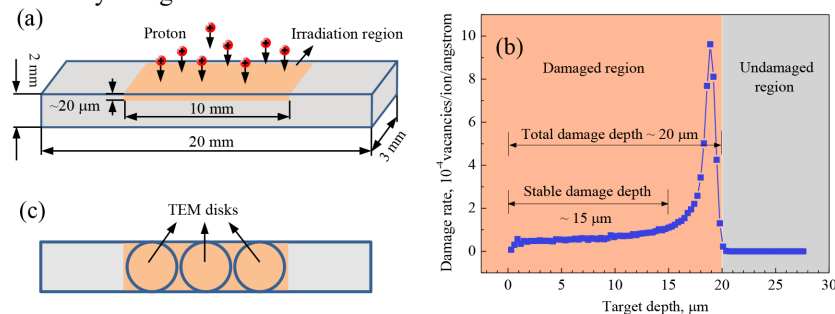
<sup>4</sup>Beijing Advanced Innovation Center for Material Genetic Engineering, University of Science and Technology Beijing, China

<sup>5</sup>Department of Nuclear Engineering and Radiological Sciences, University of Michigan

The goal of this study is to examine the effect of proton irradiation on the corrosion of austenite and  $\delta$ -ferrite phases and the respective phase boundary in 308L stainless steel weld metal in a simulated PWR environment. The results revealed that the inner oxide thickness was increased by irradiation for austenite but was largely unaffected for  $\delta$ -ferrite. This behavior was attributed to the fact that irradiation generated numerous structure defects in austenite, but not in  $\delta$ -ferrite. Following the 3 dpa irradiation, enhanced corrosion of  $\delta$ -ferrite/austenite phase boundary occurred due to the irradiation-induced Cr-depletion.  $M_{23}C_6$  carbides along the phase boundary further enhanced corrosion regardless of the irradiation condition.

All the irradiation experiments of 308L weld metal were conducted at the Michigan Ion Beam Laboratory of University of Michigan. Protons were used as the irradiation particles to simulate the neutron irradiation in service environment. During irradiation, the proton energy was accelerated up to 2 MeV, and the specimen temperature was controlled at  $360 \pm 10$  °C. Only the middle region of the specimen surface was irradiated to 0.5, 1.5 and 3 dpa at a dose rate of  $5.96 \times 10^{-6}$  dpa/s. According to the damage profile calculated by the SRIM software using Kinchin-Pease mode, a total damage depth of  $\sim 20$   $\mu\text{m}$  from the specimen surface was obtained. The recorded irradiation doses of 0.5, 1.5 and 3 dpa were all obtained at 12.3  $\mu\text{m}$ . Nevertheless, there is a platform in the depth range of about 1~15  $\mu\text{m}$  in the damage profile. In this platform, the damage rate was nearly unchanged with depth. Only in the first 1  $\mu\text{m}$  from the specimen surface, the damage rate varied greatly. As such, any depth in the platform could be applicable to a TEM observation and exposure test due to the uniform damage in this platform.

This work was supported by the National Natural Science Foundation of China (No.51771031 and No.51571204) and the International Science & Technology Cooperation Program of China (2014DFA50800). The authors are thankful to the Michigan Ion Beam Laboratory of the University of Michigan for performing proton irradiation experiments, and to the Laboratory for Microstructures of Shanghai University for performing the APT analyses and fabricating TEM and APT specimens by using FIB.



Dimension and irradiation region of the specimen. (b), damage rate profile of the irradiated specimen. (c), position of TEM disks in the irradiation region.

# STUDY OF THE RADIATION TOLERANCE OF MAB PHASES (MoAlB AND Fe<sub>2</sub>AlB<sub>2</sub>) WITH COMPARISON TO MAX PHASES

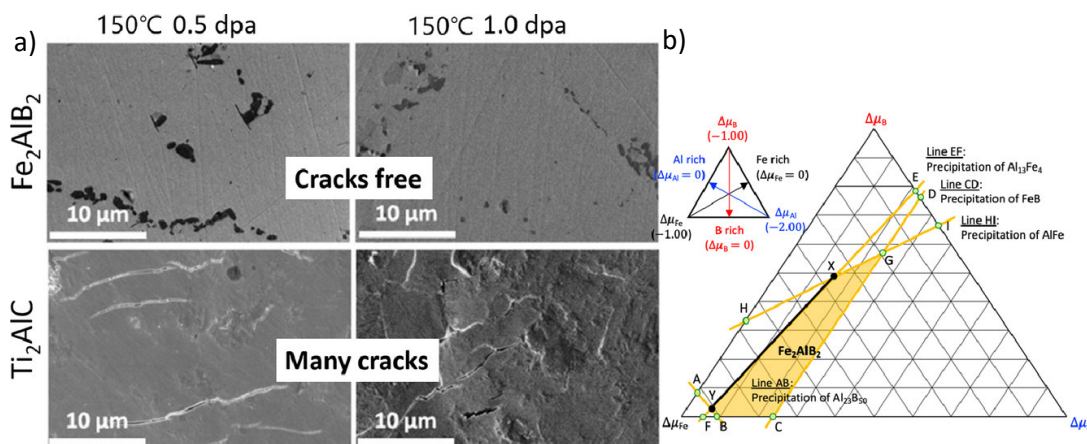
H. Zhang, J.Y. Kim, I. Szlufarska

Department of Material Science, University of Wisconsin-Madison

The goal of this study is to examine the radiation tolerance of the new series of layered ceramic material, the MAB phase. The layered ceramics have been shown to have many great properties, including thermal shock resistance, oxidation resistance, hardness, strength, and radiation resistance. Radiation effects have been studied primarily in MAX phases (M = early transition metal, A = group A element in the periodic table, and X = C or N), which in some cases can maintain their crystalline structures up to a very high radiation dose. However, the radiation-induced cracks and phase transformation limit the application of the MAX phase. MAB phases are a new class of layered ternary materials that have already shown a number of outstanding properties. While the radiation tolerance has never been studied.

Here, we investigate defect evolution and radiation tolerance of two MAB phases, MoAlB and Fe<sub>2</sub>AlB<sub>2</sub>, using a combination of experimental characterization and first-principles calculations. To examine the radiation effects, two MAB phase materials, MoAlB and Fe<sub>2</sub>AlB<sub>2</sub>, together with two MAX phase materials, Ti<sub>3</sub>SiC<sub>2</sub> and Ti<sub>2</sub>AlC were irradiated at two different temperatures with 3.15 MeV C-ion at the Michigan Ion Beam Laboratory. We find that Fe<sub>2</sub>AlB<sub>2</sub> is more tolerant to radiation-induced amorphization than MoAlB, both at 150 °C and at 300 °C. The results can be explained by the fact that the Mo Frenkel pair is unstable in MoAlB, and as a result, irradiated MoAlB is expected to have a significant concentration of MoAl antisites, which are difficult to anneal even at 300°C. We find that the tolerance to radiation-induced amorphization of MAB phases is lower than in MAX phases, but it is comparable to that of SiC. However, MAB phases do not show radiation-induced cracking which is observed in MAX phases under the same irradiation conditions. This study suggests that MAB phases might be a promising class of materials for applications that involve radiation.

This work was supported by the U.S. Department of Energy, Office of Science, Basic Energy Sciences under Award # DE-FG02-08ER46493.



SEM image (a) of Fe<sub>2</sub>AlB<sub>2</sub> and Ti<sub>2</sub>AlC after irradiation and (b) chemical potential map of Fe<sub>2</sub>AlB<sub>2</sub> with the highlighted area indicating the chemical potential ranges where MAB phases can be formed without precipitating other phases.

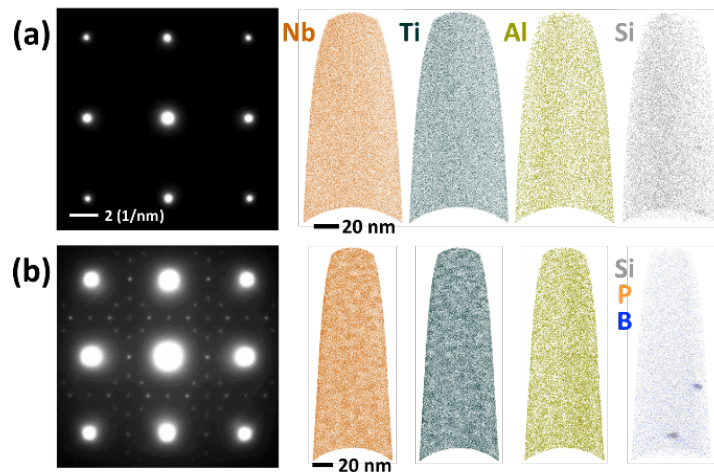
# IRRADIATION RESPONSE OF ALLOY 625PLUS

L.-J. Yu, E. Marquis

Department of Materials Science and Engineering, University of Michigan

Commercial Ni-based alloys are widely used as structural materials in nuclear power plants due to their superior high-temperature strength and corrosion resistance. However, the limitations associated with neutron irradiation experiments, such as cost, prolonged irradiation time, radioactivity issues, and limited capability of the control of experimental conditions, lead to the paucity of microstructural evolution data in Ni-based alloys. Ion and proton irradiations have been employed to facilitate the study of irradiation effects on materials' microstructures. To further infer the neutron irradiation responses using ion/proton irradiation results, differences between neutron and ion/proton irradiations, such as damage rate, cascade morphology and damage efficiency, and their potential influences on the resulting irradiated microstructures need to be understood. In addition, stability of precipitated phases and defects behavior are strongly dependent on temperature. Therefore, understanding how microstructures change with temperature is beneficial for providing thorough picture of irradiation responses of a specific alloy.

The objective of this study is to investigate the irradiation response of Alloy 625 Plus under various irradiation conditions (dose, dose rate and temperature). Solution-annealed and aged samples were irradiated at the Michigan Ion Beam Laboratory using 2 MeV protons at the dose rates of  $\sim 10^{-5}$  dpa/s or 5 MeV Ni ions at the dose rates of  $\sim 10^{-4}$  and  $\sim 10^{-3}$  dpa/s, with the dose ranging from 1.5 to 11 dpa at the temperatures of  $\sim 300$  and  $\sim 400$  °C. Microstructures including voids, dislocation loops, solute clustering, precipitates and solute segregation, were characterized using transmission electron microscopy (TEM) and atom probe tomography (APT). Results were submitted to Journal of Nuclear Materials.



$\langle 001 \rangle$ -zone TEM DPs and APT ion maps of (a) solutionized and (b) aged samples after ion irradiation at 400 °C to 3 dpa.

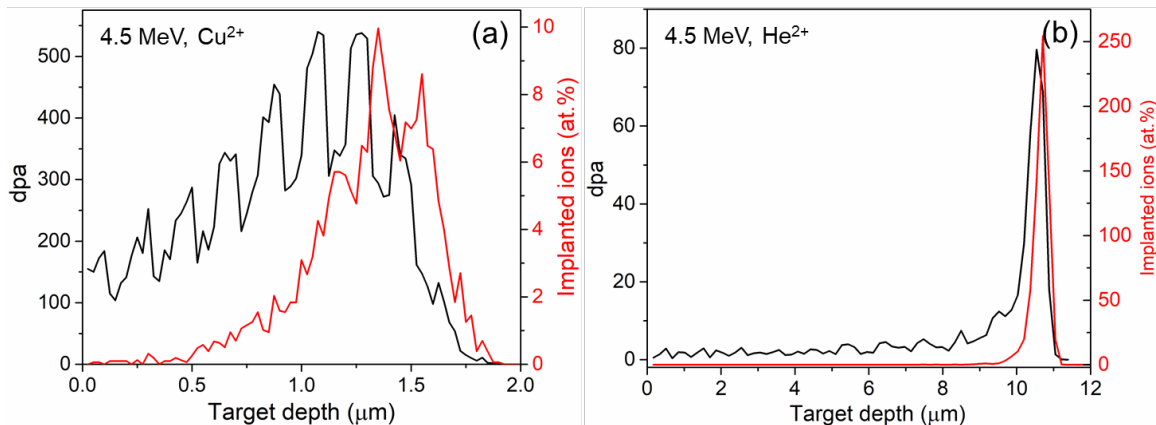
# HEAVY ION DOSE IRRADIATION OF MECHANICALLY-PROCESSED IMMISCIBLE NANOLAMINATES

M. Radhakrishnan, O. Anderoglu  
Department of Nuclear Engineering, University of New Mexico

In this work, the irradiation tolerance of immiscible laminated composites is being studied under heavy ion irradiation dose and elevated temperatures. Cu/Nb and Zr/Nb systems were chosen as the model materials for this work. Bulk laminated (multilayered) sheets were processed by accumulative roll bonding (ARB) technique, which comprises repetitive sequence of rolling, sectioning and stacking steps. The total number of layers and final layer thickness depend on the number of rolling passes in the ARB. Multilayered samples with the individual layer thicknesses ranging between 15 nm and 200 nm are being used in this work. The first part of the irradiation work is to achieve a dose up to few hundreds of dpa with self-ions at temperatures between 400 and 600°C to study the layer stability and evolution of defect structures in the multilayers under these extreme environments. The second part is to quantify the irradiation hardening of these nanolaminates by irradiating with light ions such as helium, to achieve a dose up to ~1 dpa in the uniform sub-surface damage zone.

A part of the intended heavy-ion irradiation work was performed on the Cu/Nb multilayered samples at the Michigan Ion Beam Laboratory. A defocused 4.5 MeV,  $\text{Cu}^{2+}$  ion beam was used to irradiate the samples at 600°C. The figure shows the damage profiles calculated using SRIM for the irradiation conditions employed. A maximum dose of about ~550 dpa was achieved in all the Cu/Nb samples (left). The total fluence obtained was about  $3.37 \times 10^{17}$  ions/cm<sup>2</sup> with a beam current of 383 nA. Along with Cu/Nb, pure copper sample was irradiated for comparison purpose. The ongoing work includes cross-sectional TEM/STEM characterization of the irradiated samples to study the interface morphology and defect structures.

The second set of irradiation experiment at MIBL was carried out on Zr/Nb multilayers with a light ion (right figure). A 4.5 MeV rastering beam of  $\text{He}^{2+}$  was used to irradiate the samples at 300°C. An expected average dose of 1 dpa was achieved in the constant damage depths. The total fluence obtained was about  $5.7 \times 10^{18}$  ions/cm<sup>2</sup> with a beam current of 880 nA. A pure zirconium sample was irradiated for reference. The ongoing work includes cross-sectional TEM/STEM characterization and nano-mechanical testing.



SRIM based damage and implantation profiles for the multilayers irradiated at MIBL. (a) 4.5 MeV  $\text{Cu}^{2+}$  irradiated Cu/Nb multilayers at 600°C. (b) 4.5 MeV  $\text{He}^{2+}$  irradiated Zr/Nb multilayers at 300°C.

# CALIBRATION OF THE DEPOSITION RATE OF A Ni SPUTTER TARGET

A. Ansari<sup>1</sup>, A. Sarracino<sup>1</sup>, B. Torralva<sup>2</sup>, S. Yalisove<sup>1,3</sup>

<sup>1</sup>Department of Applied Physics, University of Michigan

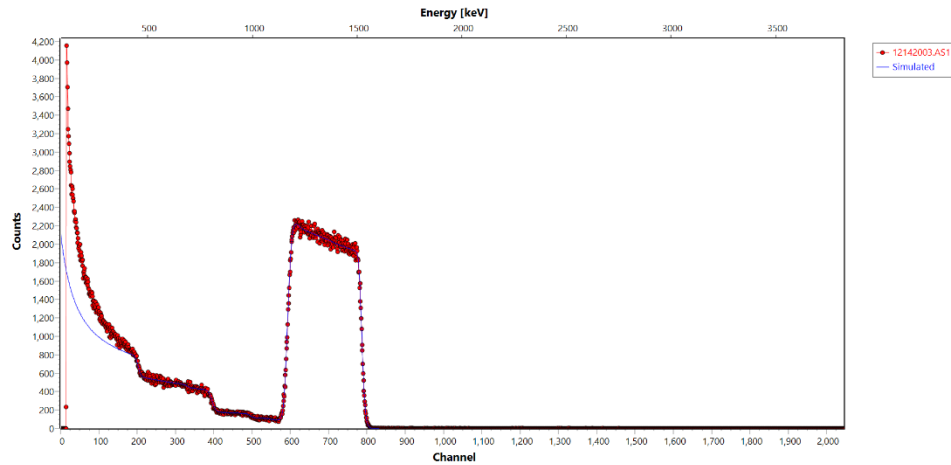
<sup>2</sup>Department of Climate and Space Sciences, University of Michigan

<sup>3</sup>Department of Materials Science and Engineering, University of Michigan

To deposit thin films of a precise thickness, the deposition rate of a sputtering system is measured when working conditions in the system have changed. One such change is the target used for the deposition, as a replacement target has a different thickness on its active area than a depleted target and may also have different mechanical properties imparted by the manufacturing process. To precisely calibrate the deposition rate, high sensitivity and low error measurement techniques are preferred. Rutherford Backscattering Spectrometry (RBS) is such a technique and can be used to calibrate sputter targets.

Helium ions at 2 MeV were incident on a nickel (Ni) film deposited using a new sputter target. A detector, at an angle of 175° relative to the incident beam, collected backscattered ions. SIMNRA was used to model and fit the collected spectrum. A sputtering rate of 0.167 nm/s was calculated.

This work is sponsored by the Air Force Office of Scientific Research Contract Number FA9550-16-1-0312.



An RBS spectrum with an accompanying fit obtained from SIMNRA. The thickness of the peak as well as the concentrations of other elements were extracted.

# REDUCING THE CONTACT RESISTANCE OF METAL-SEMICONDUCTOR JUNCTIONS FOR GALLIUM OXIDE SYSTEM THROUGH SI ION-IMPLANTATION

M.-H. Lee<sup>1</sup>, R.L. Peterson<sup>1,2</sup>

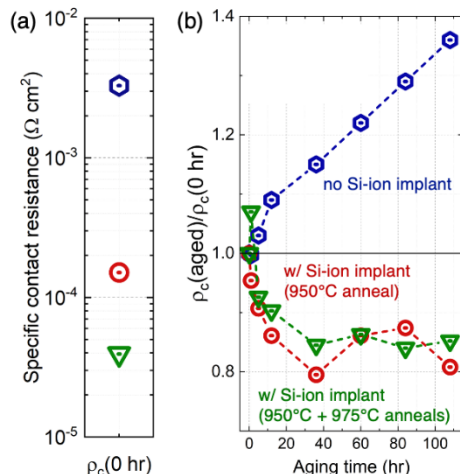
<sup>1</sup>Department of Materials Science and Engineering, University of Michigan

<sup>2</sup>Department of Electrical Engineering and Computer Science, University of Michigan

To achieve the full potential of high-power, high-frequency Ga<sub>2</sub>O<sub>3</sub> power devices, excess parasitic resistance from the metal-semiconductor junction must be aggressively reduced to minimize conduction loss. A low-resistance ohmic contact is imperative to the development of next-generation Ga<sub>2</sub>O<sub>3</sub> based electronics. The objective of this study is to enhance the ohmic properties (i.e. to minimize the contact resistance) via ion-implantation. To engineer the ohmic contact, one of the well-known methods is to degenerately dope the semiconductor to promote a tunneling pathway for charge carriers across the junction. Based on theoretical work and previous reports, in Ga<sub>2</sub>O<sub>3</sub>, silicon can act as a shallow donor, increasing the free carrier concentration. Therefore, Si ion implantation is adopted to create a heavily doped layer at the β-Ga<sub>2</sub>O<sub>3</sub> surface.

In this study, Si ions were implanted with multiple acceleration voltages and dosage conditions to create a ~180 nm/ 3x10<sup>19</sup> cm<sup>-3</sup> Si implant box profile. Post-implant anneal was performed either at a single temperature (950°C) or sequentially (950°C + 975°C) in N<sub>2</sub> environment to recover implant-induced crystalline damage and to activate the Si atoms as shallow donors. Circular Transmission Line Model structures were then fabricated on implanted and un-implanted (for comparison) samples with Ti/Au metallization. Current-voltage characteristics were measured with four-probe Kelvin configuration to characterize contact resistance of different samples. The stability of the contacts was investigated with accelerated thermal aging. A reduction in contact resistance is observed on samples with silicon ion implant. This is attributed to the heavily-doped layer, which facilitates tunneling charge transport. Accelerated thermal aging shows that the performance of the implanted samples improves while the performance of the un-implanted sample degrades over time. Results from this study pave the way for realizing and optimizing high-quality contacts for next generation Ga<sub>2</sub>O<sub>3</sub> power electronics.

This work was supported by the Department of the Navy, Office of Naval Research under ONR Award No. N00014-17-1-2998.



Room temperature contact resistance of Ti/Au – Ga<sub>2</sub>O<sub>3</sub> junctions of samples with un-implanted (blue), implanted + 950°C anneal (red), and implanted + 950°C & 975°C anneal (green) before aging (a). Evolution of contact resistance for these three samples in response to accelerated thermal aging (b). [1]

[1] Lee, M.-H. & Peterson, R. L. Accelerated Aging Stability of β-Ga<sub>2</sub>O<sub>3</sub> – Titanium/Gold Ohmic Interfaces. *ACS Appl. Mater. Interfaces* 12, 46277–46287 (2020).

# QUANTIFYING ABSOLUTE CARBON AND HYDROGEN CONCENTRATIONS IN APATITE

J. Hammerli<sup>1</sup>, F. Naab<sup>2</sup>

<sup>1</sup>Institute of Geological Sciences, University of Bern, Baltzerstrasse 1+3, CH-3012 Bern

<sup>2</sup>Department of Nuclear Engineering and Radiological Sciences, University of Michigan

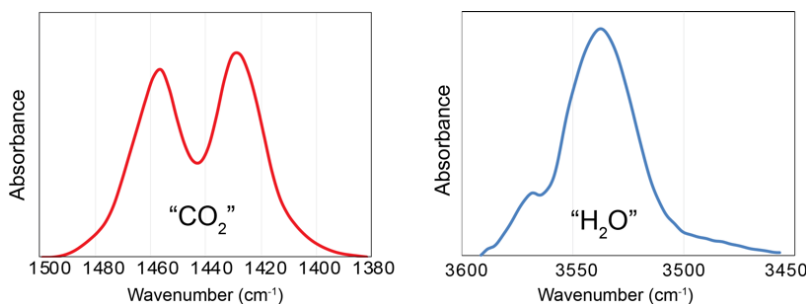
This project aims to test and characterize the carbon and hydrogen compositions of new apatite reference materials in order to calibrate micro-analytical instruments, such as Fourier-Transform Infrared Spectroscopy (FTIR), Electron Probe Micro-Analyzer (EPMA), or Secondary Ion Mass Spectrometry (SIMS). The mineral apatite ( $\text{Ca}_5(\text{PO}_4)_3(\text{F,Cl,OH})$ ), a nearly ubiquitously present accessory phase in terrestrial and extra-terrestrial rocks, can incorporate significant amounts of  $\text{CO}_2$  and  $\text{H}_2\text{O}$ , reaching weight % concentrations of either component. Apatite minerals have therefore gained attention as potential archives for  $\text{CO}_2$  and  $\text{H}_2\text{O}$  in igneous, metamorphic and hydrothermal rocks. Quantifying these volatiles in apatite holds the potential to calculate  $\text{CO}_2$  and  $\text{H}_2\text{O}$  concentrations in a variety of geological processes—a challenging endeavor—as these fugitive elements are only incorporated in a small range of minerals, yet the presence of  $\text{CO}_2$  and  $\text{H}_2\text{O}$  dictates, for example, under which temperatures the Earth's crust melts.

NRA via the 1.7 MV tandem accelerator was used to determine absolute carbon concentrations in apatite. A high-energy beam (1.4 MeV) of deuteron ( $^2\text{H}$ ) particles was used to bombard the polished apatite surface to activate the  $^{12}\text{C}$  (d,p)  $^{13}\text{C}$  nuclear reaction ( $^{12}\text{C} + ^2\text{H} \rightarrow ^{13}\text{C} + ^1\text{H}$ ). As the deuteron beam interacts with the sample,  $^2\text{H}$  particles react with the target nucleus of carbon ( $^{12}\text{C}$ ), converting the target nucleus to a new nucleus ( $^{13}\text{C}$ ), while releasing  $^1\text{H}$  as a reaction product with a specific amount of energy. The liberated  $^1\text{H}$  ions are subsequently detected in the Si charged-particle detector, set at a scattering angle of  $160^\circ$  with a 15 keV energy resolution.

ERD measurements were conducted via the 1.7 MV Tandetron accelerator. A 2.5 MeV  $\text{He}^{++}$  ion beam was used to impact the polished apatite surface from which H ions are released. Two detectors simultaneously collect the ERD and Rutherford back-scattering (RBS) spectra. The number of particle incidents on the sample during the acquisition of the ERD spectrum is measured via the RBS spectrum. A  $12.5\ \mu\text{m}$  Kapton ( $\text{H}_{10}\text{C}_{22}\text{N}_2\text{O}_5$ ) film was used in front of the ERD detector to filter out ions heavier than H. Also, a Kapton polyimide foil was used as the H standard to determine the ERD detector solid angle ( $\Delta\Omega$ ).

NRA and ERD analyses returned C contents from 0.07 to 0.72 at.% and H contents between 0.58 and 3.05 at.%. These concentrations allow us to calibrate, for example, FTIR signals (Figure 1) to absolute  $\text{H}_2\text{O}$  and  $\text{CO}_2$  concentrations.

This study is supported by Swiss National Science Foundation Grant PZ00P2\_180095, 181172 to J.Hammerli



IR peak intensities of carbonate and water in apatite. These IR absorption intensities can now be converted to absolute concentrations, determined by NRA and ERD measurements.

# **AMBIPOLAR DOPING OF RUTILE GERMANIUM OXIDE: AN ULTRAWIDE BAND GAP SEMICONDUCTOR FOR POWER ELECTRONICS**

S. Chae

Materials Science & Engineering, University of Michigan

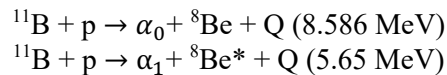
Energy-efficient power electronics is central to all social areas that utilize microelectronics. Power electronics seek to enhance energy conversion efficiency by utilizing ultra-wide-band-gap ( $> 3.4$  eV, UWBG) semiconductors with high carrier mobility and high thermal conductivity. The state-of-the-art materials are AlGaN/AlN, diamond,  $\beta$ -Ga<sub>2</sub>O<sub>3</sub>, and c-BN, but are suffering from doping asymmetry and/or thermal management, which motivates alternative UWBG semiconductors with enhanced material properties. Rutile GeO<sub>2</sub> (r-GeO<sub>2</sub>) is identified as an alternative UWBG (4.68 eV) semiconductor with predicted ambipolar doping and thermal conductivity ( $51 \text{ W m}^{-1} \text{ K}^{-1}$ ,  $\sim 3$  times higher than  $\beta$ -Ga<sub>2</sub>O<sub>3</sub>). Despite the presence of kinetically stable glass phase and high vapor pressure of GeO, I demonstrate the first synthesis of single crystal r-GeO<sub>2</sub> thin films using molecular beam epitaxy. Doping of the r-GeO<sub>2</sub> thin films by ion implantation is critical to achieve the controllable electrical property of r-GeO<sub>2</sub>. The successful demonstration of doping will provide opportunities to realize promising UWBG semiconductors with enhanced material properties to overcome the current challenges in UWBG semiconductor research.

# DETECTION OF BORON CONCENTRATION IN THIN-FILM Cr<sub>2</sub>O<sub>3</sub> FOR APPLICATIONS IN LOW POWER SPINTRONICS

N.M. Vu, J.T. Heron

Department of Materials Science & Engineering, University of Michigan

Cr<sub>2</sub>O<sub>3</sub> is one of the very few materials that exhibit magnetoelectricity at room temperature. To improve its working temperature further, boron was introduced during the fabrication processes at the 1-10% concentration levels. This project aims to detect the presence of Boron in thin-film Cr<sub>2</sub>O<sub>3</sub> (thickness ~ 60 nm, sample size 5 x 5 mm<sup>2</sup>). Detection and precise quantification of Boron have been an important but challenging task in thin-film analyses. With small doping concentrations and light atomic weight, boron detection using methods such as XPS and EELS yield an extremely low level of accuracy. Initial simulation with Rutherford scattering shows that boron signal is buried under the large background signals coming from Cr, Al, and O elements. With nuclear reaction analysis, we expect to achieve a much more accurate detection and measurement of Boron concentration in our thin-film samples. Using proton bombardment, we expect two reaction channels to happen:



The reaction channel with  $\alpha_1$  is very attractive since it shows a very sharp resonance at low incident proton energy and possesses a huge reaction cross-section at 660 kV. The challenge lies in the reactive  ${}^8\text{Be}^*$ , which will break-up to produce  $\alpha_{12}$  particles, which complicates the reaction results. Fortunately, these spectrums can be fitted to acquire the correct counts of each particle. The initial effort, however, has not shown an interpretable result. Further steps are needed for precise quantification of boron, such as fabricating control sample with known concentration and increase sample sizes (width and length) for larger particle counts while maintaining desired sample thicknesses (~ nm range).

This project is funded by SRC NewLimits Center.

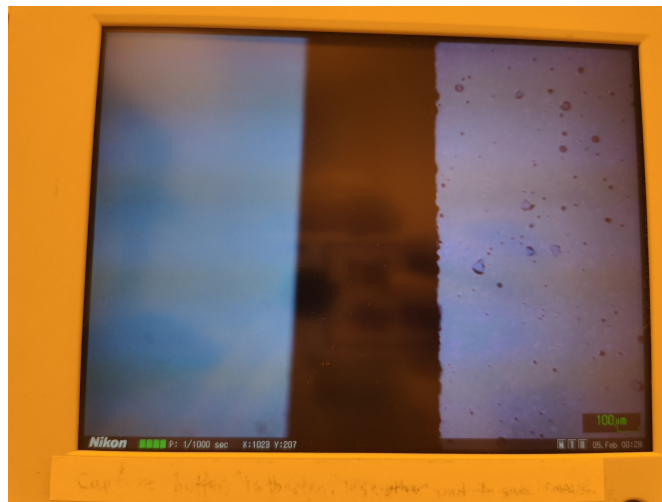
# STUDY OF SURFACE BLISTERING FORMATION USING ION IMPLANTATION

X. Zhai<sup>1</sup>, Z. Jian<sup>1</sup>, E. Ahmadi<sup>1</sup>, F. Naab<sup>2</sup>

<sup>1</sup>Department of Electrical Engineering and Computer Science, University of Michigan

<sup>2</sup>Department of Nuclear Engineering and Radiological Sciences, University of Michigan

The goal of this study is to use ion implantation to get surface blistering and finally achieve smart cut. Multiple ion implantations were conducted in MIBL. The first implantation condition was done at 300°C with 90 keV helium to  $1.5 \times 10^{17}$  i/cm<sup>2</sup> followed by 60 keV hydrogen to  $1.5 \times 10^{17}$  i/cm<sup>2</sup>. The result was not positive. As shown in the top figure, some surface damage occurs because of the high implantation temperature. This type of surface damage cannot be used for low temperature bonding. Then a second implantation was done. The condition was room temperature with 90 keV helium to  $1.5 \times 10^{17}$  i/cm<sup>2</sup> followed by 60 keV hydrogen to  $1.5 \times 10^{17}$  i/cm<sup>2</sup>. Under this condition, surface damage did not occur and the bonding was successful as shown in the bottom figure.

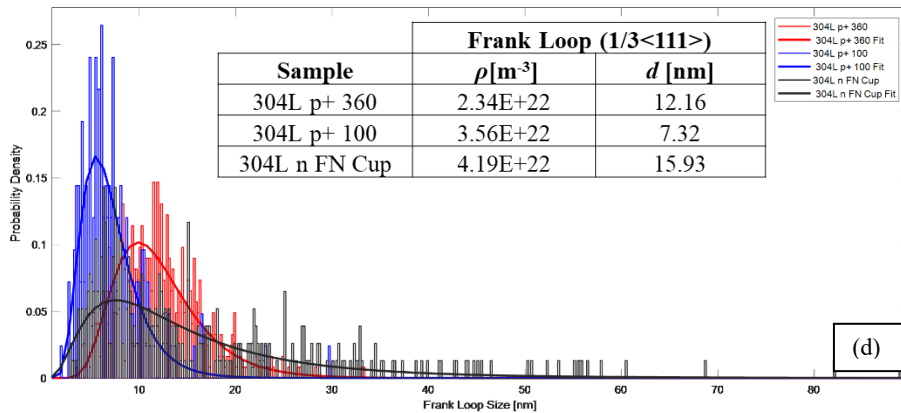
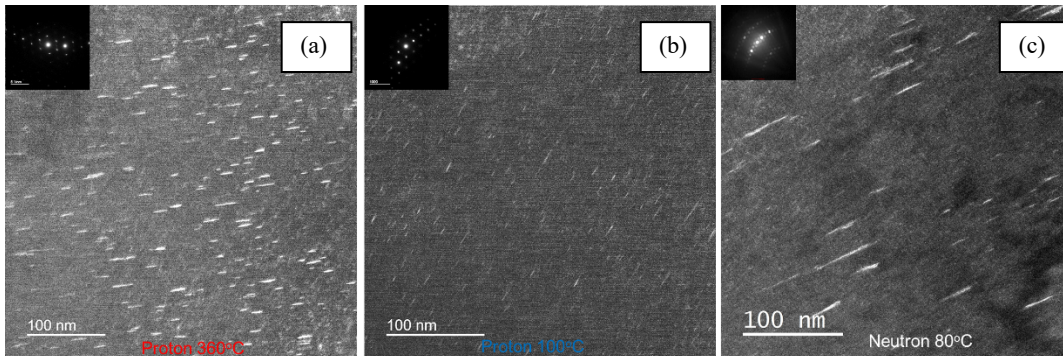


Surface damage (top) due to 90 keV helium to  $1.5 \times 10^{17}$  i/cm<sup>2</sup> followed by 60 keV hydrogen to  $1.5 \times 10^{17}$  i/cm<sup>2</sup> at 300°C. Good result (bottom) following the same implantation process but at room temperature.

# CANADIAN NUCLEAR LABORATORIES AND ACCELERATED IRRADIATIONS AT MIBL

M. Mattucci, Q. Wang J. Smith, N. Huin  
 Canadian Nuclear Laboratories (Chalk River Labs), Ontario, Canada

While much of the CANDU reactor core can be refurbished for periods of extended operations (i.e., >35 EFPY), certain key components at the core periphery, such as the calandria vessel, must remain fit for service for the total reactor lifetime. In the context of CANDU long-term operation (LTO), this could be for as long as 100 EFPY. Albeit relatively low for current reactor lifetimes, in the context of LTO, the calandria vessel is subjected to a significant neutron fluence. The combination of the unique flux spectrum and the relatively low temperature of irradiation (~80°C) is a niche issue for CANDU reactors for which some key knowledge gaps have been identified, including the effect of irradiation on mechanical properties the risk of irradiation assisted stress corrosion cracking under off-normal chemistry conditions. In addition, ex-service material is not available. Accelerated irradiation conditions were selected to try and best emulate the irradiation damage in the Calandria vessel. To address the knowledge gap that arises from no access to ex-service material, stainless steel (304L) exposed to CANDU-relevant irradiation conditions was harvested from the decommissioned NRU Reactor. The steel was subjected to a relatively high thermal neutron flux for 60 years at temperatures of <100°C. These results were compared with accelerated irradiated material from the University of Michigan as shown in the figure. This material serves as a baseline study for irradiation damage and will be used to inform future irradiations



Frank loops ( $1/3\langle 111 \rangle$ ) imaged in the rel-rod condition, for (a) p+ 360°C (b) p+ 100°C and (c) NRU Material. (d) Probability density distribution for Frank loops and mean size and density inset in table.

# RADIATION DAMAGE OF PURE METALS: HELIUM EFFECTS ON MATERIALS STRENGTH

C.R. Lear<sup>1</sup>, S.J. Fensin<sup>1</sup>, A. Llobet<sup>2</sup>

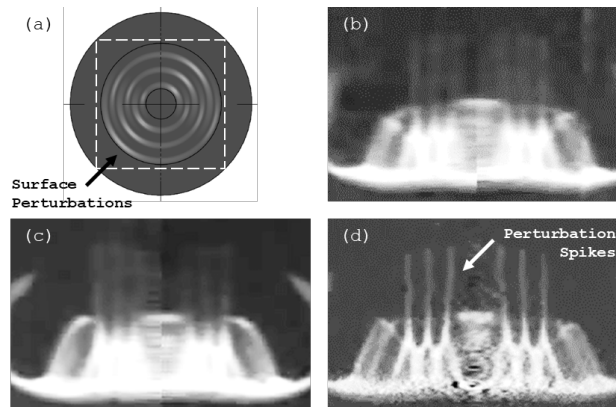
<sup>1</sup>MST-8: Materials Science in Radiation & Dynamics Extremes, Los Alamos National Laboratory

<sup>2</sup>P-1: Dynamic Imaging and Radiography, Los Alamos National Laboratory

Prolonged irradiation of metal components results in the formation of excess microstructural defects, dynamic aging, and reduced service life. The accompanying generation of helium is key to the degradation of plasma facing materials in fusion systems and to the reliability of structural materials for fission systems. Unfortunately, safety, time, and expense place limits on sample volumes for mechanical testing of irradiated materials, prohibiting large-scale mechanical testing at high temperatures and/or strain rates (e.g., 800 °C,  $10^5 \text{ s}^{-1}$ ). Considerable gaps thus exist in the available, reliable data for mechanical strength in the presence of helium defects. In this study, a series of Richtmyer-Meshkov Instability (RMI) experiments were carried out on pure metal targets, such that material strength data could be derived solely from helium implanted surface layers.

To observe the effect of helium concentration, 12 mm diameter Sn targets with sinusoidal surface perturbations, shown in the figure part a, were implanted at room temperature to 1800 and 8000 appm He. Unimplanted and implanted targets were then destructively tested at the pRad proton radiography facility at LANL, as shown in the figure parts b-d. A backing charge of high explosive (below each image) was used to produce a shockwave through each target. These shockwaves reached low points in the perturbations first, causing material to accelerate upward forming spikes. The growth rate of such spikes is a strong, if qualitative, indicator of materials strength (i.e., weaker materials grow faster), while the time-resolved growth across the experiment can be correlated to hydrodynamic materials simulations to extract more exact plasticity information. Here, however, spikes were seen to grow at nearly the same rate regardless of helium content, suggesting that high strain-rate strength is little affected by helium bubbles. While this is different from low strain-rate observations in other pure metals (e.g., yield strength increase in Ti), it is consistent with minor increases in strength observed for high strain-rate RMI experiments in helium implanted Cu. Together these findings point to a significant, if fortuitous, difference in deformation behavior between low and high strain-rate regimes that warrants further testing.

This work was supported by the U.S. Department of Energy, National Nuclear Security Administration.



Drawing (a) of tin radiography targets (12 mm  $\text{\O}$ ) with sinusoidal surface perturbations. Helium implantation areas are marked by the dashed square. (b-d) Proton radiography images 2.6  $\mu\text{s}$  after detonation for (b) 0, (c) 1800, and (d) 8000 appm He implanted. The inversion and growth of perturbation spikes with time can be correlated to materials strength.

# EVALUATION OF IRRADIATION ASSISTED STRESS CORROSION CRACKING OF NICKEL-BASE ALLOYS

P. Binks  
Jacobs Engineering

Stress Corrosion Cracking (SCC) has been known degradation mechanism for many decades and can be avoided by careful material selection and tight water chemistry control. However, exposure to a high neutron flux can cause the material to become susceptible to a phenomenon known as Irradiation-Assisted Stress Corrosion (IASCC). IASCC is typically intergranular and the amount of cracking increases with increasing neutron exposure. IASCC is an issue for existing conventional Light Water Reactor (LWR) internal components, for example, highly stressed baffle bolts for Pressurised Water Reactors (PWRs) and for the weldments in the core shroud of Boiling Water Reactors (BWRs). Typically, these components are made from 300 series austenitic stainless steel (e.g. 304 and cold worked 316). Current IASCC susceptibility databases and models are based on laboratory testing of highly neutron irradiated ex-service stainless steel components.

In recent years, there has been push away from using austenitic stainless steels for internal components for future reactor designs. A collaborative project called Advanced Radiation Resistant Materials (ARRM) managed by Electric Power Research Institute (EPRI), is currently investigating several alloys which are expected to be more superior than austenitic stainless steels, for example, a selection of low and high strength Nickel-Based Alloys (NBAs) (e.g. 625, 690, etc) along with other alloy types. No such IASCC databases and models exist for NBAs to a similar maturity as for austenitic stainless steels. Therefore, an area of research is to understand the mechanisms involved that make these alloys superior, same as or worse than austenitic stainless steels.

A practical dose of ~3 dpa at cracking can initiate above the yield stress of the material for highly stressed PWR components is used within the nuclear community. However, there is little data for IASCC susceptibility for doses <10 dpa, even for stainless steels. How this susceptibility relates to NBAs is an area of investigation. As mentioned, typically IASCC susceptibility testing is performed on neutron irradiated ex-service material. To locate neutron irradiated material at such low doses is rare, therefore, the use of ion beams to simulate neutron damage and generate material at these doses has been a practical way forward. Similar to other open research programs, the use of proton irradiation has been employed to generate material for subsequent IASCC testing.

Jacobs supplied Alloy 600 material to Michigan for proton irradiation. Alloy 600 has previously been used for bolts in the fuel assembly for PWRs and bolts in the core shroud for BWRs. Alloy 600 is known to be have a poor SCC performance and is expected to have an even worse IASCC performance. Jacobs are currently performing mechanical testing on proton irradiated 316L stainless steel using a four-point bending technique on a bespoke rig. The aim is to compare the 316L stainless steel with Alloy 600, and assess whether Alloy 600 is more or less superior than 316L stainless steel. Alloy 600 specimens supplied to Michigan have been irradiated to a nominal dose of 5 dpa, same as 316L stainless steel, to allow direct comparison. Once, the Alloy 600 material is ready to be shipped back to the UK, testing is expected to commence.

# IRRADIATION BEHAVIOR OF CONCENTRATED SOLID SOLUTION ALLOYS.

A. Kamboj, E. Marquis

Department of Materials Science and Engineering, University of Michigan

The goal of this study is to examine the effects of composition on the irradiation behavior of concentrated solid solution alloys (CSAs). As we move from dilute to concentrated solid solution alloys, there is a change in the mass transport properties of the material. The compositional complexity leads to sluggish diffusion in several CSAs. To understand the diffusion behavior in CSAs and the effect of composition, we irradiated  $\text{Cr}_{20}\text{Fe}_{40}\text{Ni}_{40}$ ,  $\text{Cr}_{18}\text{Fe}_{27}\text{Ni}_{28}\text{Mn}_{27}$ ,  $\text{Cr}_{25}\text{Fe}_{25}\text{Ni}_{25}\text{Co}_{25}$  using 6 MeV  $\text{Fe}^{3+}$  ions. The target damage for the alloys was 2dpa at 700 nm below the surface, which was achieved using  $10^{-4}$  dpa/s. The experiments were carried out using Maize accelerator and a Cu stage heated to 500°C. Temperature control was made with thermocouples, spot-welded on to the two guide bars. Thermocouple measurements were used to calibrate the thermal imaging for the temperature determination of alloys under irradiation. Temperature and beam currents were recorded during the irradiation experiments. The alloys used in the study were synthesized using arc melting and homogenized at 1200°C.

# SIMULATING NEUTRON IRRADIATION DAMAGE IN HT9 WITH HEAVY ION IRRADIATIONS

G. Bruno<sup>1</sup>, K. Sun<sup>2</sup>, K. G. Field<sup>1</sup>

<sup>1</sup>Department of Nuclear Engineering and Radiological Sciences, University of Michigan

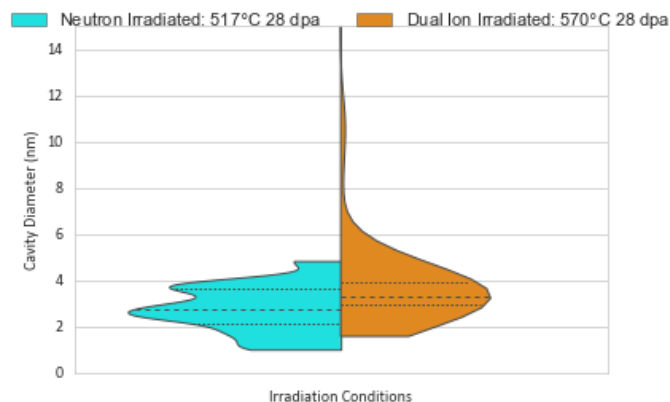
<sup>2</sup>Department of Materials Science and Engineering, University of Michigan

HT9, a ferritic-martensitic alloy, is under consideration as a structural material for advanced reactors. The testing of HT9 within materials test reactors such as the Advanced Test Reactor (ATR) could take many years or decades to reach the desired end-of-life damage levels for advanced reactor conditions. To reduce the time for testing, dual ion beams are being used to reach these damage levels in a greatly reduced amount of time. The ultimate goal of these experiments is to observe the conditions for which the microstructure from the heavy ion irradiations match the neutron irradiations.

Dual ion irradiations were run with 9 MeV Fe<sup>+++</sup> and He<sup>++</sup> with the purpose of damaging the material while simulating the production of helium within a nuclear reactor core. The irradiation conditions ranged from 445°C to 570°C with damage levels as high as 70 dpa and a 4.3 appm helium per dpa ratio. The microstructure is assessed and compared with irradiated materials from the BOR-60 fast reactor in Russia irradiated to matching conditions taking into consideration helium production and dose rate.

The samples are currently being imaged and studied at the Michigan Center for Materials Characterization at the University of Michigan - Ann Arbor for cavities, dislocation loops, and radiation induced segregation. Cavities are imaged with scanning/transmission electron microscopy (S/TEM) techniques and dislocation loops are observed using the with on-zone STEM techniques [1]. STEM-EDS maps are taken with a Thermo Fisher Talos F200X G2 S/TEM and line scans are generated from the maps to collect elemental information at the grain boundaries. Below are results comparing neutron and dual ion irradiated data of cavities for neutron irradiated HT9 at 517°C and 0.000741 dpa/s and dual ion irradiated HT9 at 570°C both at damage levels of 28 dpa. The results show a slight increase in average cavity diameter for the dual ion irradiated case, but a similar distribution in cavity sizes. Larger cavities are present in the dual ion irradiated HT9 and not in the neutron irradiated HT9.

Primary support for this research was provided by Department of Energy under contract DE-NE0000639.



Cavity diameter distribution between the high temperature neutron and dual ion irradiated HT9.

# RUTHERFORD BACKSCATTERING SPECTROMETRY/CHANNELING MAPS OF GaN SURFACES

J. He<sup>1</sup>, G. Cheng<sup>1</sup>, Z. Zhang<sup>1</sup>, A. Zimmerman<sup>1</sup>, S. Frisone<sup>1</sup>, F. Naab<sup>2</sup>, R.S. Goldman<sup>1</sup>, S. Wang<sup>3</sup>, B. Li<sup>3</sup>, J. Han<sup>3</sup>

<sup>1</sup>Materials Science and Engineering, University of Michigan

<sup>2</sup>Nuclear Engineering and Radiological Sciences, University of Michigan

<sup>3</sup>Electrical Engineering, Yale University

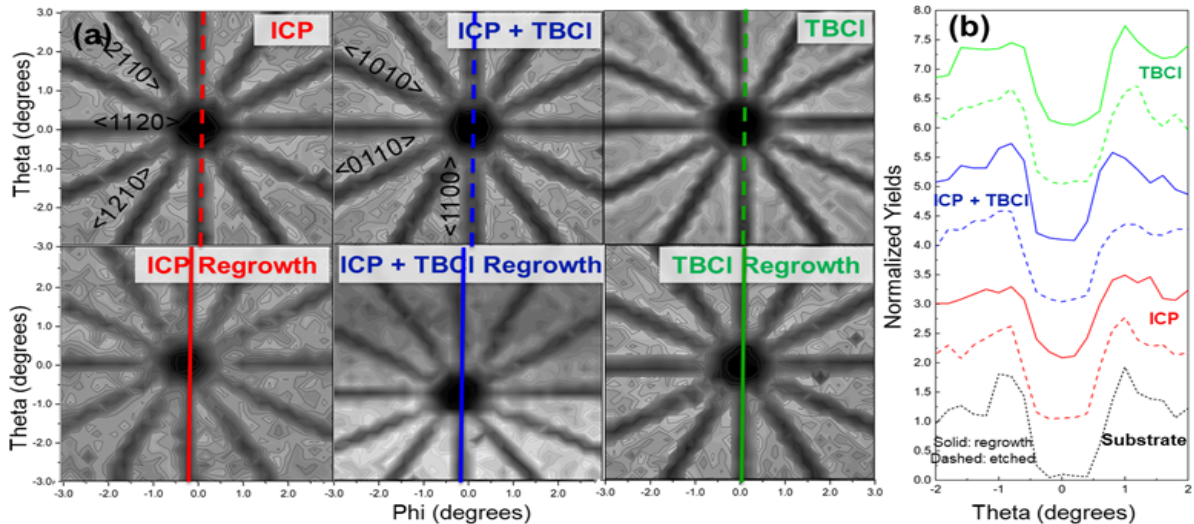
To understand processing-structure-property relationships relevant to vertical GaN devices, we examine the influence of ex-situ dry etching (ICP) and in-situ tertiarybutylchloride (TBCl) treatments on the structure and properties of GaN substrates and overgrown epitaxial GaN layers. We use Rutherford Backscattering Spectrometry channeling (RBS/c) maps to visualize the 12-fold symmetry [Fig. part a]. Following overgrowth, the [0001] channel is narrowed, suggesting displacement of Ga into the channel. To quantify the fraction of displaced Ga,  $N_d/N$ , and the average Ga displacement,  $r_x$ , we extracted angular yield profiles about  $\theta$  [Fig. part b]. Using minimum yields for the pristine GaN substrate [ $\chi_0$ ] and those following each chemical treatment/overgrowth [ $\chi_{min}$ ],  $N_d/N$  becomes

$$\frac{N_d}{N} = \frac{\chi_{min} - \chi_0}{1 - \chi_0}$$

To compute  $r_x$ , we extract full-widths at half depths, i.e. at  $\frac{1 - \chi_{min}}{2}$ , for both the pristine GaN substrate ( $\Psi_0$ ) and those following each chemical treatment/overgrowth ( $\Psi_{sample}$ ), assuming a constant ( $C \sim \sqrt{3}$ ), thermal vibrational amplitude ( $\rho = 0.062 \text{ \AA}$ ), and Thomas-Fermi screening radius ( $a = 1.73 \text{ \AA}$ ), to solve

$$\frac{\Psi_{sample}}{\Psi_0} = \frac{\ln [(Ca/r_x)^2 + 1]}{\ln [(Ca/\rho)^2 + 1]}$$

For the pristine GaN substrate,  $N_d/N \sim 0$  with  $r_x \sim 0.062 \text{ \AA}$ . Following ICP and ICP+TBCl etching,  $N_d/N$  increases to  $< 0.006$ , while  $r_x$  increases to  $\sim 0.0634 \text{ \AA}$ . Following overgrowth, ICP “regrowth” and ICP+TBCl “regrowth”,  $N_d/N$  increases to  $\sim 0.066$ , while  $r_x$  increases to  $\sim 0.07 \text{ \AA}$ . Interestingly, TBCl etched and “regrowth” both have  $N_d/N \sim 0.042$  and the lowest  $r_x \sim 0.0622 \text{ \AA}$ . These results suggest that TBCl provides the lowest  $N_d/N$  and  $r_x$  of the overgrown layers.



(a): RBS/c maps about [0001] for etched GaN substrates (top) and overgrown GaN layers (bottom), with lowest yields shown as dark regions. The channels were identified by rotating the goniometer in steps of  $0.2^\circ$  in  $\theta$  and  $\phi$ . For each RBS/c map, the yields are integrated over the top 100nm; normalization is achieved by dividing the counts at each point by the average counts from the entire map. The dashed and solid vertical lines in (a) are used to select out the (b)  $\langle 110 \rangle$  angular yield profiles for the substrates and overgrown layers.

# ION AND ELECTRON IRRADIATION OF Gd-SIM FOR ISOLATION OF ACTINIDES

K. Sun<sup>1</sup>, G.S. Was<sup>2</sup>

<sup>1</sup>Materials Science and Engineering, University of Michigan  
Nuclear Engineering and Radiological Sciences, University of Michigan

A gadolinium-containing salt inclusion material (Gd-SIM) of composition  $(K_9F_2)(Gd_3Si_{12}O_{32})$  was exposed to ion and electron irradiation in an effort to determine its stability against amorphization prior to the incorporation of actinides. Samples were in the form of lift-outs of thickness  $<100$  nm and mounted on a DENSolutions Wildfire in-situ heating stage for irradiation in an FEI 300 kV Tecnai G2 F30 transmission electron microscope. Xenon  $3+$  ions of energy 1.2 MeV were used to irradiate the sample *in-situ* in the TEM over a range of damage rates spanning 3 orders of magnitude at both room temperature and 400°C. At room temperature, the sample was amorphized at a damage level of  $\sim 0.09$  dpa irrespective of damage rate. At 400°C, the amorphization dose was found to be similar over most of the same damage range but a damage rate dependence was observed at the lowest damage rate as shown in the left figure.

Irradiation of the Gd-SIM with a 300 keV electron beam was conducted at room temperature over a range of fluxes that varied by a factor of 80. At both the lowest ( $6 \times 10^{17}$  e<sup>-</sup>/cm<sup>2</sup>s) and highest ( $5 \times 10^{19}$  e<sup>-</sup>/cm<sup>2</sup>s) flux, the sample was observed to be completely amorphized by a fluence of  $\sim 5 \times 10^{21}$  e<sup>-</sup>/cm<sup>2</sup>. Figure 2 shows a series of high resolution images of the sample at different levels of exposure to the highest electron beam flux of  $5 \times 10^{19}$  e<sup>-</sup>/cm<sup>2</sup>s; crystalline structure prior to exposure (Fig. 2a), strain-induced lattice distortion (upper right), formation of cavities (lower left), and partial amorphization after 70 s of exposure (Fig. 2b), and complete amorphization after 120 s (Fig. 2c). Amorphization caused a volume increase of at least 28%.

Results indicate that the Gd-SIM is easily amorphized by both displacement-dominated damage (Xe ions) and by ionization (electrons) at relatively low dpa and electron doses, respectively. With either particle, there was no observable damage rate or flux effect at room temperature, and only a mild damage rate effect at 400°C for ion irradiation at the lowest damage rate.

Support for this research was provided by the Department of Energy under contract DE-SC0016574 / 21-4258.

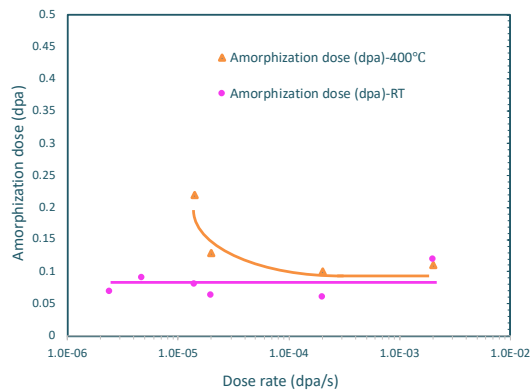
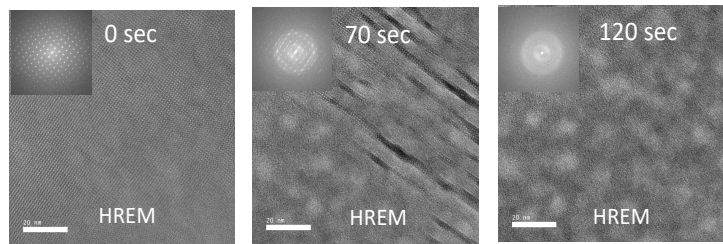


Figure 1. Dose to amorphization of Gd-SIM irradiated with 1.2 MeV Xe<sup>3+</sup> over a range of damage rates at both room temperature and 400°C.



High resolution images of Gd-SIM following irradiation with 300 keV electrons in-situ in the TEM; crystal planes prior to irradiation (left), formation of strain-induced lattice distortion, cavities and partial amorphization after 70 s (center), and complete amorphization after 120 s (right).

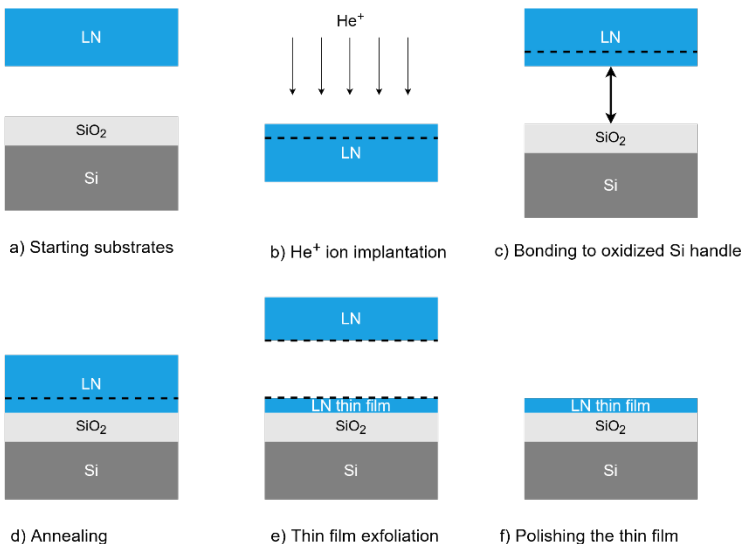
# FABRICATION OF THIN-FILM LITHIUM NIOBATE ON INSULATOR THROUGH ION-SLICING

Karan Prabhakar, Ryan J. Patton, and Ronald M. Reano  
 ElectroScience Laboratory, Department of Electrical and Computer Engineering,  
 The Ohio State University

Photonic integrated circuits utilize electro-optic waveguide devices that frequently employ ferroelectric materials such as lithium niobate (LN). LN is attractive due to its strong nonlinear susceptibility and high electro-optic coefficient. Thin ferroelectric films less than a micron thick are especially advantageous for waveguide devices due to the reduced mode effective area leading to enhanced electro-optic effects, such as making  $\chi^{(2)}$  nonlinearity observable at low optical power levels. Among the various methods used to incorporate LN into waveguide devices, a preferred approach is to bond LN thin films to an insulating material with a lower refractive index than LN, such as silicon dioxide. The insulating layer forces most of the optical power to be confined to the LN thin film. This layered structure is often referred to as lithium niobate on insulator (LNOI). In this project, we utilize the ion-slicing method to fabricate LN thin films bonded to thermally oxidized Si wafers.

Magnesium oxide doped LN wafers are implanted with  $\text{He}^+$  ions at an energy of 225 keV which introduces a damage layer approximately 800 nm below the surface as predicted by TRIM simulations. The implanted LN wafer is bonded to a thermally oxidized Si carrier and annealed at elevated temperature. Increased temperature causes helium blisters to form at the damage layer. At sufficient temperatures and durations, layer splitting occurs which leaves a wafer-scale LN thin film bonded to the Si carrier. Wafers implanted at MIBL will subsequently be bonded and annealed to achieve film exfoliation, and finally be polished to sub-nanometer RMS surface roughness as required for optical devices. The polished films will be used in fabrication of electro-optic waveguide devices. Additional implantations at MIBL are planned for this project.

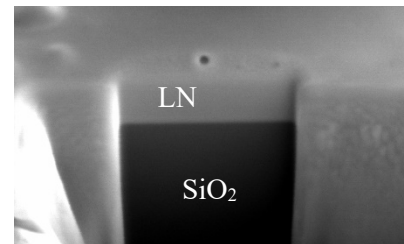
This research is supported by the National Science Foundation under Award No. 1809894.



(a) Starting with a 3-inch LN wafer and an oxidized Si substrate, (b) the LN wafer is implanted with  $\text{He}^+$  ions and (c) bonded to the Si handle. (d) The stack is subsequently annealed which leads to (e) thin film being exfoliated. (f) The sample is finally chemo-mechanically polished.



LN wafer temporarily bonded to an aluminum carrier via silver paste inside the implantation chamber



Scanning electron micrograph of LN thin film cross-section using a FIB milled trench.

# Teaching

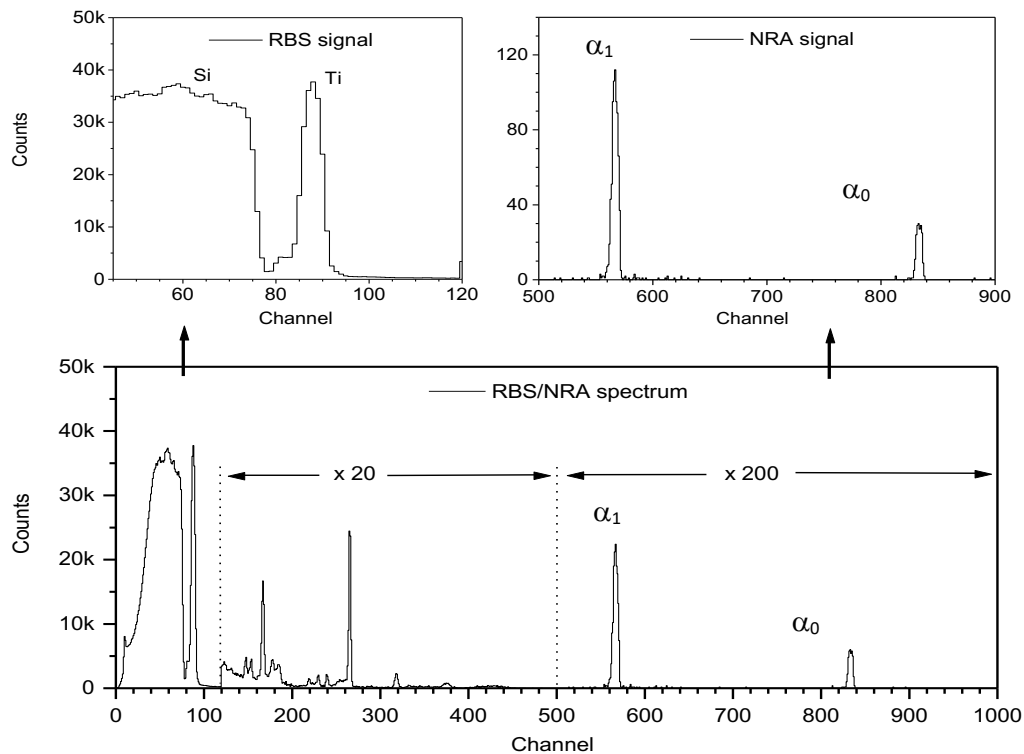
# NERS 425 LABORTORY ON NUCLEAR REACTION ANALYSIS

M. Atzmon, F. Naab and O. Toader

Department of Nuclear Engineering and Radiological Sciences, University of Michigan

For one of the modules in the NERS 425 course, students conducted an experiment to determine the stoichiometry of a  $Ti_xN_y$  sample using the reaction between a deuterium particle and a nitrogen nucleus:  $N^{14}(d,\alpha)C^{12}$ . Nuclear reaction analysis (NRA) is a well-established surface analysis technique. In this method, an energetic particle (deuterium – produced by the Tandem accelerator at MIBL) interacts with the nucleus of an N atom in the target to give a reaction product ( $\alpha$  particle) that can be measured. The students also use the backscattered yield from an RBS experiment to determine the amount of Ti in the sample by implementing simulation codes like RUMP or SIMNRA with the given experimental spectrum.

In the first meeting, prior to the experiment, a short tutorial was given to the students on the accelerator, electronics, detectors, software, and vacuum components. After that, they worked independently with just the basic support from the MIBL staff (required in the setup of the ion beam and the collection of the spectra). The students decided on a few parameters of the experiment (beam energy, time for spectrum acquisition, etc.), and obtained spectra similar to the ones in the figure.



Typical RBS/NRA spectrum for the TiN film obtained during class. Conditions: beam energy: 1.4 MeV  $D^+$ , solid angle 5 msr., detector angle  $150^\circ$ .

## PUBLICATIONS AND PRESENTATIONS

### Publications

1. S. Taller, G. S. Was, "Understanding Bubble and Void Nucleation in Dual Ion Irradiated T91 Steel using Single Parameter Experiments," Acta. Mater. 198 (2020) 47-60.
2. M. Song, K. G. Field, R. M. Cox, G. S. Was, "Microstructural Characterization of Cold-Worked 316 Stainless Steel Flux Thimble Tubes Irradiated up to 100 dpa in a Commercial Pressurized Water Reactor," J. Nucl. Mater. 541 (2020) 152400.
3. S. Taller, F. Naab, G. S. Was, "A Methodology for Customizing Implantation Profiles of Light Ions using a Single Thin Foil Energy Degradation," Nucl. Instr. Meth. Phys. B. 478 (2020) 274-283.
4. G. S. Was and S. J. Zinkle (2020). Toward the Use of Ion Irradiation to Predict Reactor Irradiation Effects. In: Konings, Rudy JM and Stoller Roger E (eds.) Comprehensive Nuclear Materials 2nd edition, vol. 1, pp. 468-484. Oxford: Elsevier.
5. P. Wang, S. Grdanovska, D. M. Bartels, G. S. Was, "Effect of Radiation Damage and Water Radiolysis on Corrosion of FeCrAl Alloys in Hydrogenated Water," J. Nucl. Mater. 533 (2020) 152108.
6. W. Kuang, G. S. Was, "The Effect of Grain Boundary Structure on the Intergranular Degradation Behavior of Solution Annealed Alloy 690 in High Temperature Hydrogenated Water," Acta. Mater. 182 (2020) 120-130.
7. B. Khur, D. Farkas, I. M. Robertson, D. Johnson, G. Was, "Stress Localization Resulting from Grain Boundary Dislocation Interactions in Relaxed and Defective Grain Boundaries," Metall. Mater. Trans. A. 51 (2020) 667-683.

### Presentations

1. G. S. Was, "Insights into Factors Controlling IASCC of Stainless Steels," Symposium on Environmentally Assisted Cracking: Theory and Practice, 2020 TMS Annual Meeting, San Diego, February, 2020.
2. G. S. Was, "Capturing the Multiple Components of the Reactor Core Environment for Materials Development," Physics/Theory Colloquium Series, Los Alamos National Laboratory, New Mexico, January, 2020.